สารยับยั้งโคลีนเอสเทอเรสจากมะกรูด *Citrus hystrix* DC.

นายเศรษฐกร เนียมเที่ยง

วิทยานิพนธ์นี้เป็นส่วนหนึ่งของการศึกษาตามหลักสูตรปริญญาวิทยาศาสตรมหาบัณฑิต
สาขาวิชาเคมี ภาควิชาเคมี
คณะวิทยาศาสตร์ จุฬาลงกรณ์มหาวิทยาลัย
ปีการศึกษา 2556
ลิขสิทธิ์ของจุฬาลงกรณ์มหาวิทยาลัย

CHOLINESTERASE INHIBITORS FROM *Citrus hystrix* DC.

Mister Setthakorn Niamthiang

A Thesis Submitted in Partial Fulfillment of the Requirements

for the Degree of Master of Science Program in Chemistry

Department of Chemistry

Faculty of Science

Chulalongkorn University

Academic Year 2013

Thesis Title   CHOLINESTERASE INHIBITORS FROM *Citrus hystrix* DC.

By   Mister Setthakorn Niamthiang

Field of Study   Chemistry

Thesis Advisor   Assistant Professor Pattara Sawasdee, Ph.D.

Accepted by the Faculty of Science, Chulalongkorn University in Partial Fulfillment of the Requirements for the Master's Degree

……………………………………… Dean of the Faculty of Science

(Professor Supot Hannongbua, Dr. rer. nat.)

THESIS COMMITTEE

……………………………………… Chairman

(Assistant Professor Warinthorn Chavasiri, Ph.D.)

……………………………………… Thesis Advisor

(Assistant Professor Pattara Sawasdee, Ph.D.)

……………………………………… Examiner

(Associate Professor Santi Tip-pyang, Ph.D.)

……………………………………… External Examiner

(Assistant Professor Wimolpun Rungprom, Ph.D.)

เศรษฐกร เนียมเที่ยง : สารยับยั้งโคลีนเอสเทอเรสจากมะกรูด *Citrus hystrix* DC. (CHOLINESTERASE INHIBITORS FROM *Citrus hystrix* DC.) อ.ที่ปรึกษาวิทยานิพนธ์หลัก : ผศ.ดร.พัฒทรา สวัสดี, 71 หน้า.

ได้สารบริสุทธิ์ 10 ชนิดจากสิ่งสกัดใบและรากของมะกรูด โดยพิสูจน์ทราบโครงสร้างของสารที่แยกได้ทั้งหมดด้วยเทคนิคเอ็น เอ็ม อาร์ และเปรียบเทียบกับรายงานที่ได้ตีพิมพ์แล้ว ซึ่งได้แก่ hesperidin (1) และ neohesperidin (2) จากสิ่งสกัดบิวทานอล alkyl alcohol (3) และ oxypeucedanin hydrate (4) จากสิ่งสกัดไดคลอโรมีเทนของใบมะกรูด สิ่งสกัดรากมะกรูดได้สาร limonin (5) xanthyletin (6) crenulatin (7) 5-hydroxynoracronycine (8) citracridone-I (9) และ umbelliferone (10) สารที่แยกได้ทั้งหมดถูกนำไปทดสอบฤทธิ์ยับยั้งแอซีทิลโคลีนเอสเทอเรสและบิวทิริลโคลีนเอสเทอเรส ผลการทดสอบพบว่าสารส่วนใหญ่มีค่าการยับยั้งในช่วงต่ำไปจนถึงปานกลางและแสดงการยับยั้งเพิ่มขึ้นเมื่อมีการเพิ่มความเข้มข้นของสารตัวอย่าง ค่า IC_{50} ของ neohesperidin (2) ต่อแอซีทิลโคลีนเอสเทอเรสเท่ากับ 160.1 ไมโครโมลาร์ และค่า IC_{50} ของ oxypeucedanin   hydrate (4) ต่อบิวทิริลโคลีนเอสเทอเรสเท่ากับ 260.8   ไมโครโมลาร์ xanthyletin (6) มีฤทธิ์ในการยับยั้งต่อโคลีนเอสเทอเรสสูงที่สุด โดยมีค่า IC_{50} ต่อแอซีทิลโคลีนเอสเทอเรสเท่ากับ 116.2   ไมโครโมลาร์และค่า IC_{50} ติอบิวทิริลโคลีนเอสเทอเรสเท่ากับ 37.4 ไมโครโมลาร์ และแสดงการยับยั้งแบบผสมจากการศึกษาทางจลนศาสตร์ต่อบิวทิริลโคลีนเอสเทอเรส งานวิจัยนี้ได้รายงานฤทธิ์ในการยับยั้งต่อเอนไซม์บิวทิริลโคลีนเอสเทอเรสและการยับยั้งแบบผสมของ xanthyletin เป็นครั้งแรก

ภาควิชา_____เคมี_____ลายมือชื่อนิสิต_____

สาขาวิชา_____เคมี_____ลายมือชื่อ อ.ที่ปรึกษาวิทยานิพนธ์หลัก_____

ปีการศึกษา____2556____

\# \# 5272686023 : MAJOR CHEMISTRY

KEYWORDS : *Citrus hystrix* DC. / RUTACEAE / ACETYLCHOLINESTERASE / BUTYRYLCHOLINESTERASE

SETTHAKORN NIAMTHIANG: CHOLIENESTERASE INHIBITORS FROM *Citrus hystrix* DC. ADVISOR : ASST. PROF. PATTARA SAWASDEE, Ph.D., 71 pp.

Ten compounds were obtained from the leaf and root extracts of *Citrus hystrix*. Structural elucidation of all isolated compounds were performed by NMR data and compared with the published data. Hesperidin (**1**) and neohesperidin (**2**) were afforded from the BuOH extract whereas alkyl alcohol (**3**) and oxypeucedanin hydrate (**4**) were also obtained from the dichloromethane extract of *C. hystrix* leaves. The root extract of this plant gave limonin (**5**), xanthyletin (**6**), crenulatin (**7**), 5-hydroxynoracronycine (**8**), citracridone-I (**9**) and umbelliferone (**10**). All isolated compounds were tested for their anti-acetylcholinesterase (AChE) and butyrylcholinesterase (BChE) activities. The results found that most of them showed low to moderate inhibition in dose-dependent manners. The IC_{50} value towards AChE of neohesperidin (**2**) was 160.1 μM, and that of oxypeucedanin hydrate (**4**) towards BChE was 260.8 μM. Xanthyletin (**6**) showed the highest inhibition towards AChE and BChE with IC_{50} value of 116.2 and 37.4 μM, respectively, with a mixed inhibitory mode towards BChE. The BChE inhibitory activity and mode of inhibition of xanthyletin were reported for the first time.

Department : .... Chemistry .... Student's Signature ....

Field of Study : ...... Chemistry .... Advisor's Signature ....

Academic Year : .... 2013 ....

ACKNOWLEDGEMENTS

CONTENTS

LIST OF TABLES

LIST OF FIGURES

LIST OF SCHEMES

LIST OF ABBREVIATIONS

br s	=	broad singlet (NMR)
BuOH	=	butanol
C	=	carbon
^{13}C-NMR	=	carbon-13 nuclear magnetic resonance
CHCl$_3$	=	chloroform
J	=	coupling constant
acetone-*d$_6$*	=	deuterated acetone
C. hystrix	=	*Citrus hystrix*
chloroform-*d$_1$*	=	deuterated chloroform
CH$_2$Cl$_2$	=	dichloromethane
d	=	doublet (NMR)
dd	=	doublet of doublet (NMR)
ESI-MS	=	electrospray ionization mass spectroscopy
EtOAC	=	ethyl acetate
U	=	enzyme unit
g	=	gram
Hz	=	hertz (NMR)
H	=	hydrogen
OH	=	hydroxy group
kg	=	kilogram
MHz	=	megahertz (NMR)
Me	=	methyl
MeOH	=	methanol
OMe	=	methoxy group
μL	=	microliter

μM	=	micromolar
mg	=	milligram
mL	=	milliliter
mM	=	millimolar
min	=	minute
M	=	molarity
m	=	multiplet (NMR)
ppm	=	part per million
%	=	percentage
^{1}H-NMR	=	proton-1 nuclear magnetic resonance
n	=	sample size (statistic)
sat. BuOH	=	saturated butanol
s	=	singlet (NMR)
S.D.	=	standard deviation (statistic)
t	=	triplet (NMR)
δ	=	unit of chemical shift
$δ_C$	=	chemical shift of carbon
$δ_H$	=	chemical shift of proton
UV	=	ultraviolet
v	=	volume
H_2O	=	water

CHAPTER I

INTRODUCTION

Alzheimer's disease (AD) is a progressive and neurodegenerative disease which is the most common form of dementia affecting in the elderly persons over 65 years old. Presently, this disease has become the fourth leading cause of death in developed country. The Alzheimer's Disease International has estimated that about 115.4 million people will suffer from AD in 2050 (Alzheimer's Disease International, 2010). AD is not only characterized by memory impairment, but also results in functional and behavioral disturbances, deterioration of language, visuospatial deficits, sensory abnormalities, gait disturbances, and seizures (Cummings, 2004). Three current hypotheses of AD, neurotransmitter acetylcholine deficiency, senile plaques, and Alzheimer's neurofibrillary tangles, are the major lesion characteristic of AD. Nowadays, there is currently no cure for this disease. Pharmacotherapy is only focused on symptomatic profit and delaying disease progression. Moreover, the pathophysiology of AD is not yet nearly clarified and under investigation.

Successful treatments for central nervous system disorder have been developed from European and Oriental medicinal plants relied on some folk cultural, believes, and religions. For examples, essential oil from the Spanish sage *Salvia lavandulaefolia* (Lamiaceae) had anti-cholinesterase and memory-enhancing activities (Tildesley *et* al, 2003). Ginkgo *Ginkgo biloba* extract (Ginkgoaceae) were testified capably in clinical trials for AD treatment (Gertz and Kiefer, 2004). Furthermore, galantamine obtained from the flowers of the Caucasian snowdrop *Galanthus woronowii* (Amaryllidaceae) (Heinrich and Teoh, 2004), and huperazine A obtained from club moss *Huperzia serrate* (Lycopodiaceae) (Frank and Gupta, 2005) showed high anti-cholinesterase activity and also inhibited formation of β-amyloid peptide fragment. These are acceptable example of plant secondary compounds favourably used for the treatment of AD. The studies for the natural source medicines for the treatment of AD are global progressing processes especially in Thailand. For

instance, the leaves of Champaca *Michelia champaca* (Magnoliaceae) are used in the treatment of brain disorders (Clayton *et al.*, 1994). Moreover, a screening test of some Thai herbs for cholinesterase inhibitory properties showed that some herbs, stephania *Stephania suberosa* (Menispermaceae), black pepper *Piper nigrum* (Piperaceae), sakhan *Piper interruptum* (Piperaceae), crape jasmine *Tabernaemontana divericata* (Apocynaceae), and red kwao krua *Butea superba* (Fabaceae) inhibited cholinesterases at medium to high levels (Ingkaninan *et al.*, 2003).

There are a number of Thai herbs that still remain unscreened. The preliminary test of more than ten extracts of Thai herbs revealed that the extract from leaves and roots of *Citrus hystrix* also showed the significant cholinesterase inhibition. Interstingly, there are still no publication reported the cholinesterase inhibitory activity from the leaves and roots extracted. Consequently, the aims of this research were to investigate the components from *C. hystrix* extracted and evaluated their anti-cholinesterase activities. This study will revealed the advantages and phytochemical information to the development of Thai herbal medicine for the therapy of AD and other neurodegenerative disorder as well.

1.1 Botanical Properties and Distribution of *Citrus hystrix*

Citrus hystrix DC. (Rutaceae) is a native plant in South-east Asia, especially in Thailand, Malaysia, and Indonesia. Its common names are kaffir lime, ma-krut (Thai) or jeruk purut (Indonesian and Malaysian). The *C. hystrix* leaves commonly used for decorating and flavoring in South-east Asian cuisine, e.g. soups, stews, curries, and sauces. Local Indonesians use the young fruits for sore throat treatment and the leaf paste for headache remedy (Elliott and Brimacombe, 1987). The botanical properties of *C. hystrix* can be described as follows:

Tree: Thorny bush, typically grow 3 to 6 metres.

Leaves: Evergreen, aromatic leaf, distinctive shape, double form with a more pointed top leaf joined to a more round bottom leaf.

Flowers: Round buds open into fragrant flowers with 4 to 5 petals and around 30 stamens, petals are white with pink on the outside.

Fruits: Rough skin with small numerous oil glands, bumpy green fruit, from 3 to 5 cm wide by 5 to 7 cm long.

(a)   (b)

Figure 1.1 leaf (a), and fruits (b) of *C. hystrix*

1.2 Literature Reviews of *Citrus hystrix*

Extracts and essential oils from many parts of *C. hystrix* exhibited a variety of biological activities. The chloroform extract of leaves inhibited implantation, produced abortion, enhanced the uterotropic effect of estradiol and stimulated uterine contractions (Piyachatuwat *et al.*, 1985). The methanol extract of fruits inhibited Herpes simplex type 1 (HSV-1) (Fortin *et al.*, 2002), scavenged radicals DPPH and ferric ion in FRAP assay (Wong *et al.*, 2006). Moreover, this extract showed photo-cytotoxic activity towards human leukaemia cell-line HL-60 (Ong *et al.*, 2009). Essential oil from leaves possessed anti-bacterial activity towards *Clostridium perferingens* (Wannisorn *et al.*, 2005,) and in *vitro* acetylcholinesterase inhibitory activity (Chaiyana *et al.*, 2010; Chaiyana and Okonogi, 2012). In addition, essential oils have moderate anti-proliferative activity towards human mouth epidermal carcinoma (KB) and murine leukemia (P388) cell lines (Manosroi *et al.*, 2006).

There are many classes of active compounds isolated from *C. hystrix*. Two glyceroglycolipids; 1,2-di-*O*-α-linolenoyl-3-*O*-*β*-galactopyranosyl-*sn*-glycerol and 1-*O*-α-linolenoyl-2-*O*-palmitoyl-3-*O*-*β*-galactopyranosyl-*sn*-glycerol   (Figure   1.2), isolated from the methanol extract showed potent inhibition towards tumor promoter-induced Epstein-Barr virus (EBV) with lower IC_{50} values than that of cancer preventive agents (Murakami *et al.*, 1995a; Murakami *et al.*, 1995b).
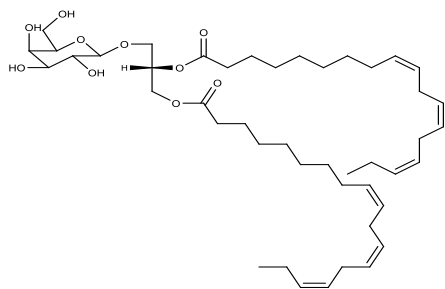
1,2-di-*O*-α-linolenoyl-3-*O*-β-galactopyranosyl-*sn*-glycerol
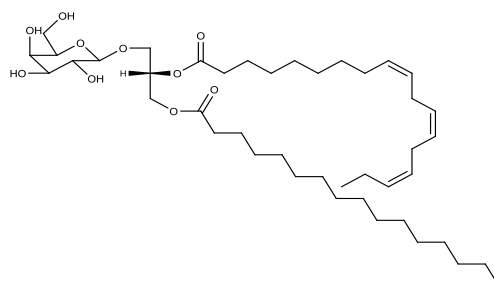
1-*O*-α-linolenoyl-2-*O*-palmitoyl-3-*O*-β-galactopyranosyl-*sn*-glycerol
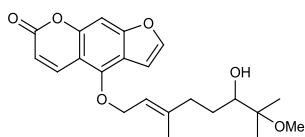
6′-hydroxy-7′-methoxybergamottin
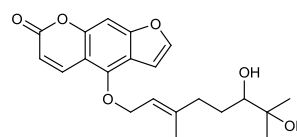
6′,7′-dihydroxybergamottin
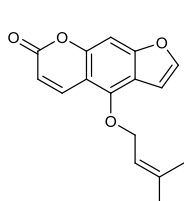
isoimperatorin
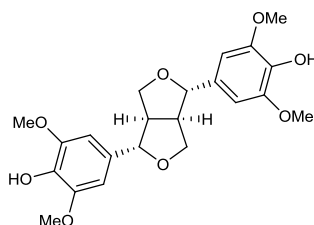
syringaresinol
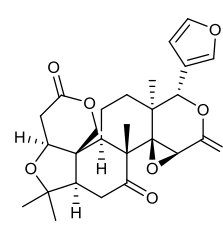
limonin
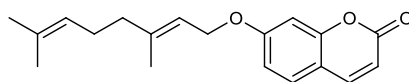
auraptene
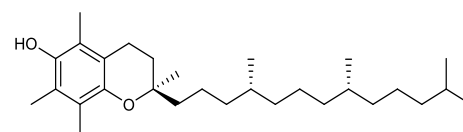
α-tocopherol
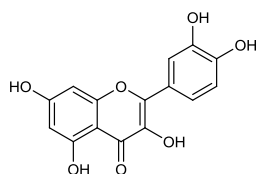
quercetin
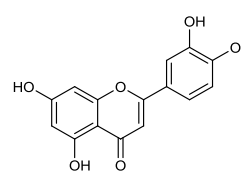
luteolin

Figure 1.2 Isolated compounds from *C. hystrix*

The structure activity relationship study of coumarins isolated from *C. hystrix* revealed that coumarins bearing an isoprenyl (IP) or a geranyl (GR) group showed high inhibitory effect towards lipopolysaccharide (LPS) and interferon-γ (IFN-γ)-induced nitric oxide (NO) generation in RAW 264.7 cells (Murakami *et al.*, 1999). In addition, 6′-hydroxy-7′-methoxybergamottin, 6′,7′-dihydroxybergamottin, and isoimperatorin (Figure 1.2) isolated from the fruit peel of *C. hystrix* showed high inhibitory activity towards butyrylcholinesterase (Youkwan *et al.*, 2010).

Aromatic compounds, coumarins and quinolinone derivatives isolated from the roots of this plant exhibited anti-oxidant, anti-HIV and anti-bacterial activities (Figure 1.2) (Panthong *et al.*, 2013). Furthermore, auraptene, α-tocopherol, quercetin and luteolin (Figure 1.2) were additionally obtained from the roots of *C. hystrix* (Ogawa *et al.*, 2000; Ching and Mohamed, 2001; Miean and Mohamed, 2001).

1.3 Cholinesterase Inhibitory Activities

Genetic factor, mutation of amyloid precursor protein (APP), and non-genetic factors, aging and oxidative stress, are possible pathogenesis of AD. The abnormal processing and increased of amyloid precursor protein from these factors influence the deposition of senile plaques and Alzheimer's neurofibrillary tangle that disturb the metabolism of neurotransmitter acetylcholine (Ach). ACh is involved in neuropsychic activities, such as memory, movement and learning. Choline acetyltranferase (ChAT) responses for the formation of the acetylcholine (ACh) in the pre-synaptic neuron. This neurotransmitter leaves the neuron and binds to the receptor causing the signal to be sent (Figure 1.3), following with a hydrolysis by acetylcholinesterase at the cholinergic synapse to yield choline and acetate (Scheme 1.1). Acetylcholinesterase (AChE) and butyrylcholinesterase (BChE) are widely distributed in a variety of tissues in many species, including human. The main function of AChE is rapid hydrolysis of neurotransmitter acetylcholine, whereas BChE catalysed the hydrolysis of a wide variety of choline, such as butyrycholine, succinylcholine, and non-choline esters (Atack *et al.*, 1986). The previous studies revealed that BChE bares some structural similarities to AChE, likewise metabolizes acetylcholine (Darvesh *et al.*, 2003). In the cerebral neocortex and hippocampus of Ad patients, the reduction of

acetylcholine and ChAT activity is significantly correlated with the amount of neurofibrillary tangles (Oda, 1999). Moreover, AChE activity is significantly lower as well, ranging from 62 to 67% of the normal value. Conversely, BChE activity is substantially increased to 140 to 165% of the normal level (Perry *et al.*, 1978). These observations correlated to a cholinergic hypothesis, which stated that cognitive, functional abnormalities associated with defective cholinergic neurotransmission.
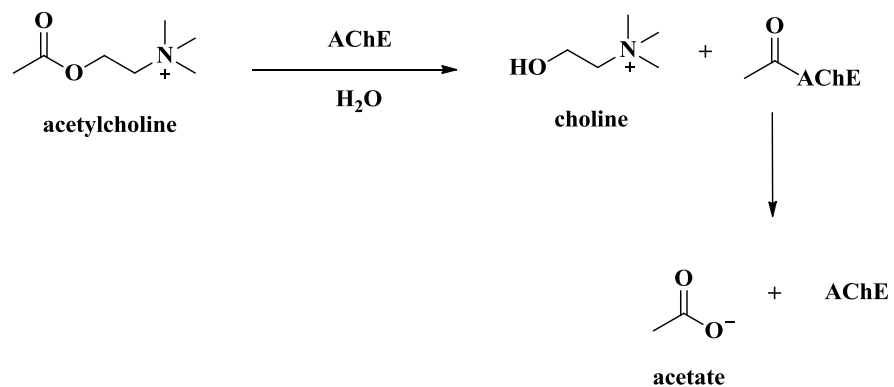
Scheme 1.1 The reaction during the hydrolysis of acetylcholine
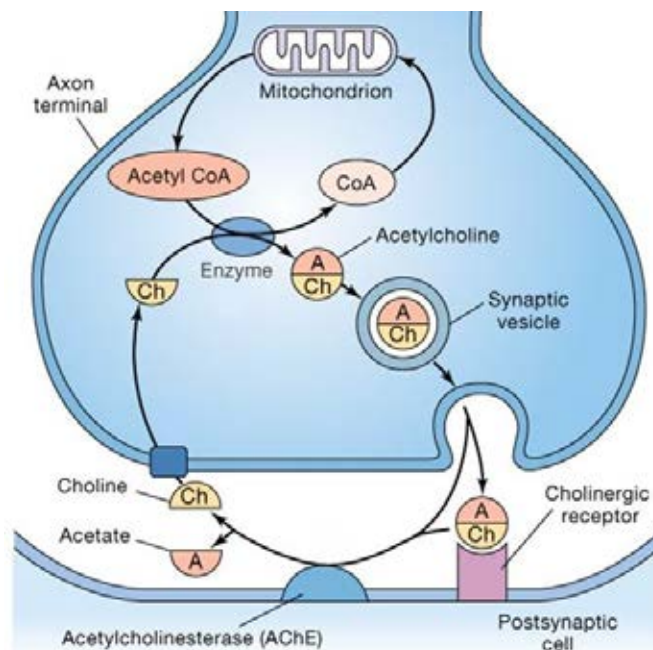
Figure 1.3 The action mechanism of acetylcholinesterase

(http://faculty.pasadena.edu/dkwon/chap%208_files/images/image61.png)

Therapeutic agents, the most effective, widely studied, developed approach and currently used to treat AD are cholinesterase inhibitors. The reason for their use is that the relatively selective loss of cortical acetylcholine, and the action of them is believed to increased and prolong the availability of acetylcholine, therefore improving cognition. Most inhibitors have been focused on inhibition of AChE, but BChE might be important to inhibit in the treatment of AD. BChE inhibitors are not only improve cognition, but also reduce levels of the amyloid precursor protein (Darvesh *et al.*, 2003). So, therapeutic agents that serve as inhibitors of both AChE and BChE could provide additional advantages in the treatment of AD.

There are four FDA-approved drugs, tacrine, donepezil, galantamine, and rivastigmine (Figure 1.4), that improve symtoms by inhibiting AChE. Tacrine is now infrequently used, as it has the dose-dependent hepatotoxic effects. Donepezil, a selective inhibitor of AChE, is initiated at a dose of 5 mg per day, and increased to 10 mg per day after one month, usually administered at bedtime, due to its long pharmacokinetic and pharmacidynamic half-life. With generally few side effects, donepezil held the most outstanding position in AD market share. Rivastigmine is a co-inhibitor both AChE and BChE, unlike the other approved agents. The dose of it increases from 1.5 mg twice daily to 3 mg twice daily, then to 4.5 mg twice daily, and to a maximal dose of 6 mg twice daily, increased to 8 mg twice a day and to 12 mg twice daily. Side effects observed in clinical trials included nausea, vomiting and diarrhea, as well as insomnia, abnormal dream, weight loss, bradycardia, synrope, muscle cramps and fatigue. These effects occurred during the initiation of treatment, reduced with slower rates of drug titration and during maintenance therapy (Lahiri *et al.*, 2002). So, the research for a potent, long-term both AChE and BChE inhibition with minimal side effects at therapeutic dose for the treatment of AD is still ongoing.

tacrine (Cognex®)   donepezil (Aricept®)

galantamine (Razadyne®)   rivastigmine (Exelon®)
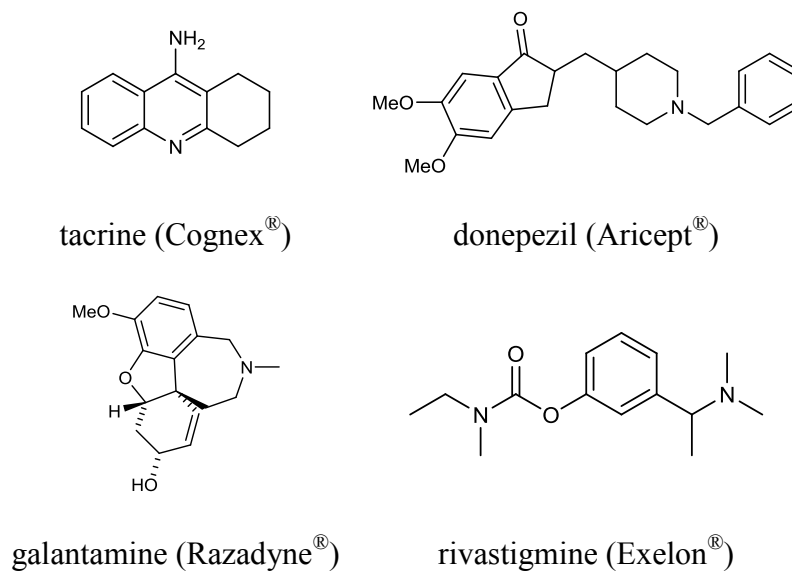
Figure 1.4 The FDA-approved drugs

1.4 The Goals of This Research

1.4.1 Extract and isolate the chemical constituents from the leaves and roots of *Citrus hystrix*.

1.4.2 Elucidate the structures of the isolated compounds form the leaves and roots of *Citrus hystrix*.

1.4.3 Evaluate the anti-cholinesterase activities of the isolated compounds from the leaves and roots of *Citrus hystrix*.

CHAPTER II

EXPERIMENTAL

2.1 Plant Materials

The leaves and roots of *C. hystrix* were collected in May 2012 from Chonburi Province, Thailand and identified by Assoc. Prof. Nijsiri Ruangrungsi, Faculty of Pharmaceutical Sciences, Chulalongkorn University. A voucher specimen (No. NPRU 0002) has been deposited in the Natural Products Research Unit, Department of Chemistry, Faculty of Science, Chulalongkorn University, Thailand.

2.2 Instruments and Equipment

The ^{1}H NMR (at 400 MHz) and ^{13}C NMR spectra (at 100 MHz) were recorded in dueterated solvents, e.g. chloroform-d_1 (CDCl$_3$), acetone-d_6 (C$_3$D$_6$O), methanol-d_4 (CD$_3$OD) and DMSO-d_6 ((CD$_3$)$_2$SO), on a Bruker Advance 400 and a Varian model Mercury+ 400 NMR spectrometer. To isolate and purify active compounds, silica gel 60 (particle size: 0.063-0.200 mm and particle size 0.040-0.063 mm for flash column, Merck), Sephadex LH-20 (Amersham Pharmacia Biotech), and thin layer chromatography precoated silica gel (silica gel 60 F$_{254}$, Merck) were used. The spots on plates were detected under a UV light at 254 and 365 nm.

2.3 Extraction Procedure of *C. hystrix* Leaves and Roots

The dried leaves of *C. hystrix* (0.8 kg) were ground and extracted three times with methanol at room temperature. The extract solution was concentrated under reduced pressure, and subsequently partitioned with hexane, dichloromethane (CH$_2$Cl$_2$) and saturated *n*-butanol yielding hexane (17.2 g), dichloromethane (6.5 g), and *n-butanol* (9.1 g) extracts, respectively. The extraction procedure of *C. hystrix* leaves is summarized as displayed in Scheme 2.1.

The dried roots of *C. hystrix* (1.9 kg) were ground and extracted three times with EtOAc at room temperature. After remove solvent under reduced pressure, 20 g of EtOAc extract was obtained. The extraction procedure of *C. hystrix* roots is summarized as displayed in Scheme 2.2.

Dried leaves of *C. hystrix* (0.8 kg)

Maceration with MeOH

MeOH extract
(150.5 g)

Marc

Partition with *n*-hexane

n-hexane extract
(17.2 g)

MeOH layer

Partition with CH_2Cl_2

MeOH layer

CH_2Cl_2 extract
(6.5 g)

Partition with sat. BuOH

BuOH extract
(9.1 g)

Aqua layer
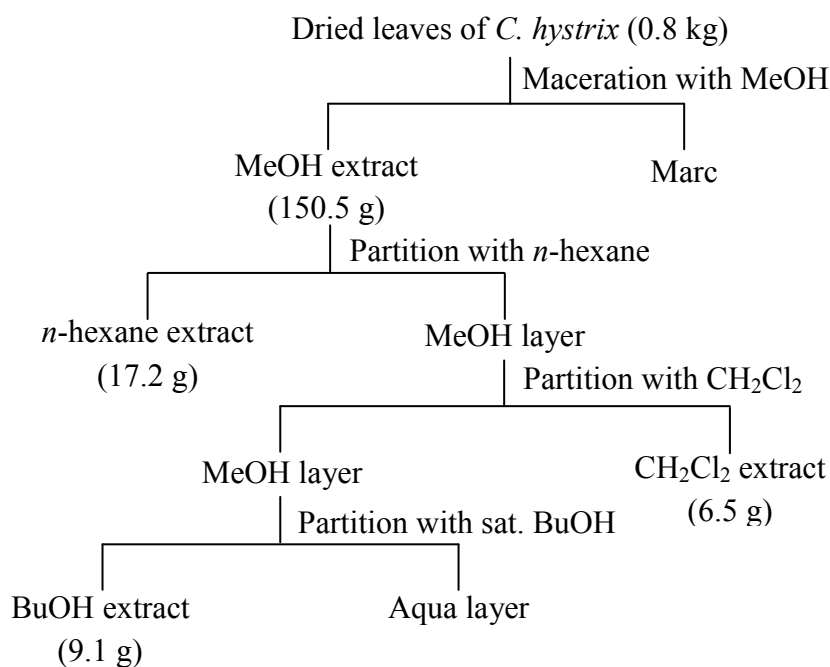
Scheme 2.1 Extraction procedure of *C. hystrix* leaves

Dried roots of *C. hystrix* (1.9 kg)

Maceration with EtOAc

EtOAc extract
(20.2 g)

Marc
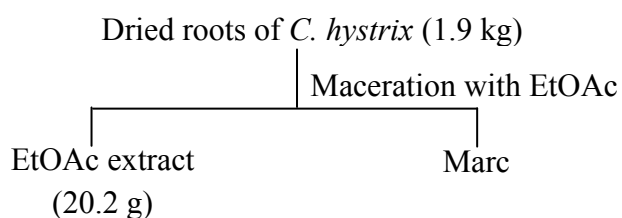
Scheme 2.2 Extraction procedure of *C. hystrix* roots

All extracts were evaluated for their preliminary anti-cholinesterase activities using microplate and TLC-autobiography assays.

2.4 Separation and Isolation Chemical Constituents from the Leaves Extract of *C. hystrix*

The butanolic extract (8.5 g) was subjected to vacuum silica gel column chromatography (VCC) with a gradient system of hexane:EtOAc and EtOAc:MeOH by increasing polarity. Each fraction was combined monitoring by TLC analysis to give 7 sub-fractions (KB1 to KB7). Fraction KB2 was further separated by a silica gel column using a gradient system of hexane:EtOAc and then EtOAc:MeOH to obtain six sub-fractions (KB2.1 to KB 2.6). Subfraction KB2.2 was re-chromatographed on a silica gel column with a gradient system of hexane:EtOAc and EtOAc:MeOH to obtain six sub-fractions (KB2.2.1 to KB 2.2.6). Subfraction KB2.2.3 was purified by a sephadex LH-20 column eluting with MeOH to give hesperidin (**1**) (5.4 mg). Sub-fraction KB2.2.4 was purified by a sephadex LH-20 column eluting with MeOH to yield neohesperidin (**2**) (40.6 mg). The isolation diagram of butanolic extract is presented in Scheme 2.3.

A portion of CH$_2$Cl$_2$ extract (5.0 g) was subjected to a silica gel column with a gradient system of hexane:EtOAc and then EtOAc:MeOH to obtain three sub-fractions (KD1 to KD3). Fraction KD2 was chromatographed on a silica gel column using a gradient system of hexane:EtOAc and EtOAc:MeOH to give six sub-fractions (KD2.1 to KD2.6). Subfraction KD2.3 was re-chromatographed on a silica gel column with a gradient system of hexane:EtOAc to yield alkyl alcohol (**3**) (170.2 mg). Sub-fraction KD2.4 was further fractionated using a silica gel column eluting with a gradient system of hexane:EtOAc to yield six sub-fractions (KD2.4.1 to KD2.4.6). Sub-fraction KD2.4.3 was purified with a silica gel column using a gradient system of hexane:EtOAc and recrystallized with EtOAc to give oxypeucedanin hydrate (**4**) (30.3 mg). The separation diagram of dichloromethane extract is described in Scheme 2.4.

Butanolic extract

Vacuum silica gel CC

KB1   KB2   KB3   KB4   KB5   KB6   KB7

Silica gel CC   KB1   KB1   KB1   KB1

KB2.1   KB2.2   KB2.3   KB2.4   KB2.5   KB2.6

Silica gel CC

KB2.2.1   KB2.2.2   KB2.2.3   KB2.2.4   KB2.2.5   KB2.2.6

Sephadex   Sephadex

| Compound **1** (5.4 mg) | Compound **2** (40.6 mg) |
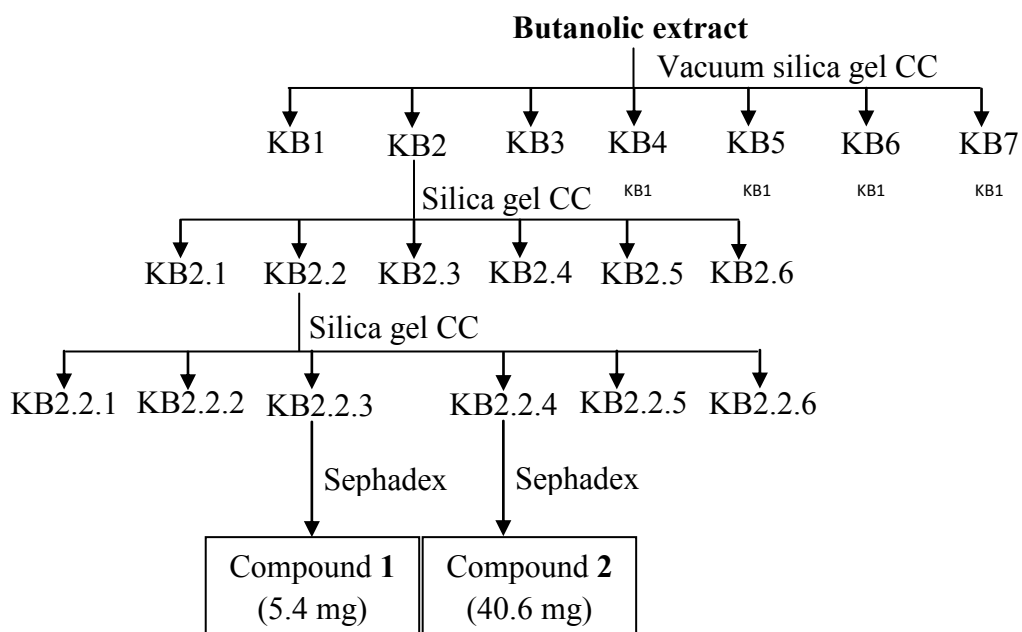
Scheme 2.3 The isolation diagram of butanolic extract from leaves of *C. hystrix*

CH$_2$Cl$_2$ extract

Vacuum silica gel CC

KD1   KD2   KD3

Silica gel CC

KD2.1   KD2.2   KD2.3   KD2.4   KD2.5   KD2.6

Silica gel CC

KD2.4.1   KD2.4.2   KD2.4.3   KD2.4.4   KD2.4.5   KD2.4.6

Silica gel CC   Silica gel CC

| Compound **3** (170.2 mg) | Compound **4** (30.3 mg) |
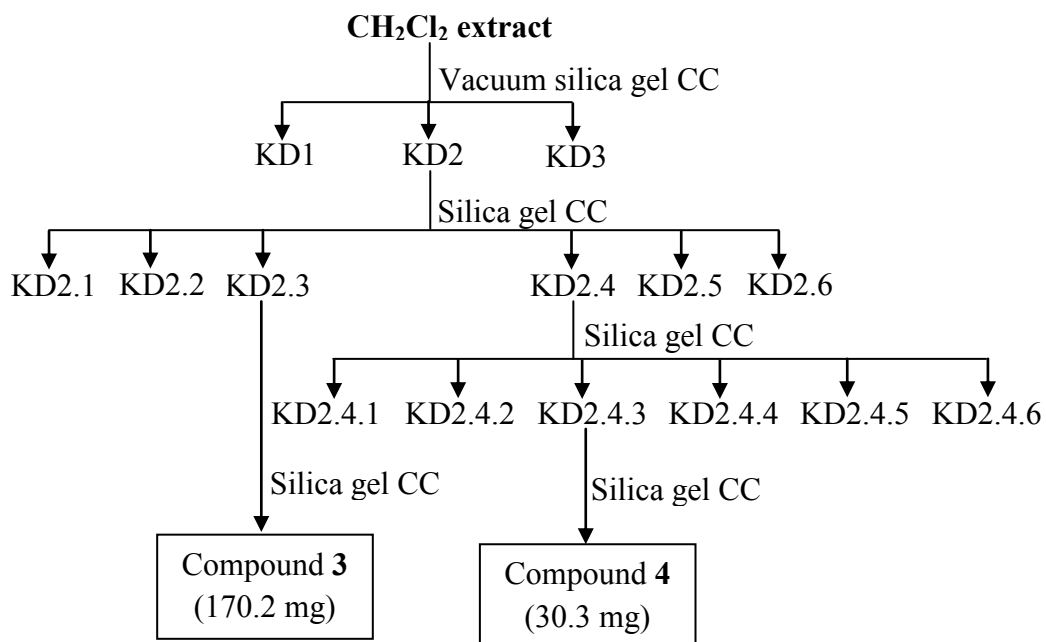
Scheme 2.4 The isolation diagram of dichloromethane extract from leaves of

C. hystrix

2.5 Separation and Isolation Chemical Constituents from the Root Extract of *C. hystrix*

The EtOAc extract (10.2 g) from the *C. hystrix* roots was fractionated by a silica gel VCC with a gradient system of hexane:EtOAc and EtOAc:MeOH to obtain five sub-fractions (RE1 to RE5). Limonin (**5**) (250.2 mg) was afforded after re-crystallization fraction RE4 with EtOAc. Sub-fraction RE3 was chromatographed on a sephadex LH-20 column using chloroform:MeOH (1:1, v/v) as eluent to give four sub-fractions (RE3.1 to Re3.4). Sub-fraction RE3.3 was further chromatographed on a flash silica gel column using a gradient system of hexane:EtOAc to yield twenty-eight sub-fractions (RE3.3.1 to RE3.3.28). Sub-fraction RE3.3.3 was recrystallized with hexane:EtOAc (8:2, v/v) to give xanthyletin (**6**) (211.5 mg). Sub-fraction RE3.3.12 was purified with a sephadex LH-20 column eluting with chloroform:MeOH (1:1, v/v) to yield crenulatin (**7**) (2.1 mg) and 5-hydroxynoracronycine (**8**) (2.4 mg). Sub-fraction RE3.3.13 was re-chromatographed on a sephadex LH-20 column eluting with chloroform:MeOH (1:1, v/v) to give citracridone-I (**9**) (2.2 mg). Sub-fraction RE3.3.15 was purified on a sephadex LH-20 column eluting with chloroform:MeOH (1:1, v/v) to give umbelliferone (**10**) (2.3 mg). The isolation diagram of EtOAc extract is described in Scheme 2.5.

The structures of these isolated compounds were fully elucidated on 1D NMR data and comparison with those of published data. Moreover, all isolated compounds were evaluated their anti-cholinesterase activities towards acetyl- and butyryl-cholinesterase.

```
                        EtOAc extract
                    |Vacuum silica gel CC
        ┌───────┬─────────────┼─────────────────┬──────┐
        ↓       ↓              ↓                 ↓      ↓
      RE1     RE2            RE3               RE4    RE5
                         |Sephadex
                ┌──────┬─────┬──────┐
                ↓      ↓     ↓      ↓
             RE3.1  RE3.2 RE3.3  RE3.4
                     |Flash silica gel CC
        ┌──────────┬─────────┬──────────┐
        ↓          ↓         ↓          ↓
     RE3.3.3   RE3.3.12  RE3.3.13   RE3.3.15
```

Crystallized (RE4 → Crystallized)

Sephadex (RE3.3.12)   Sephadex (RE3.3.13)   Sephadex (RE3.3.15)

Crystallized (RE3.3.3)

| Compound **6** (211.5 mg) |

| Compound **9** (2.2 mg) |

| Compound **5** (250.2 mg) |

| Compound **10** (2.3 mg) |

| Compound **7** (2.1 mg) | Compound **8** (2.4 mg) |
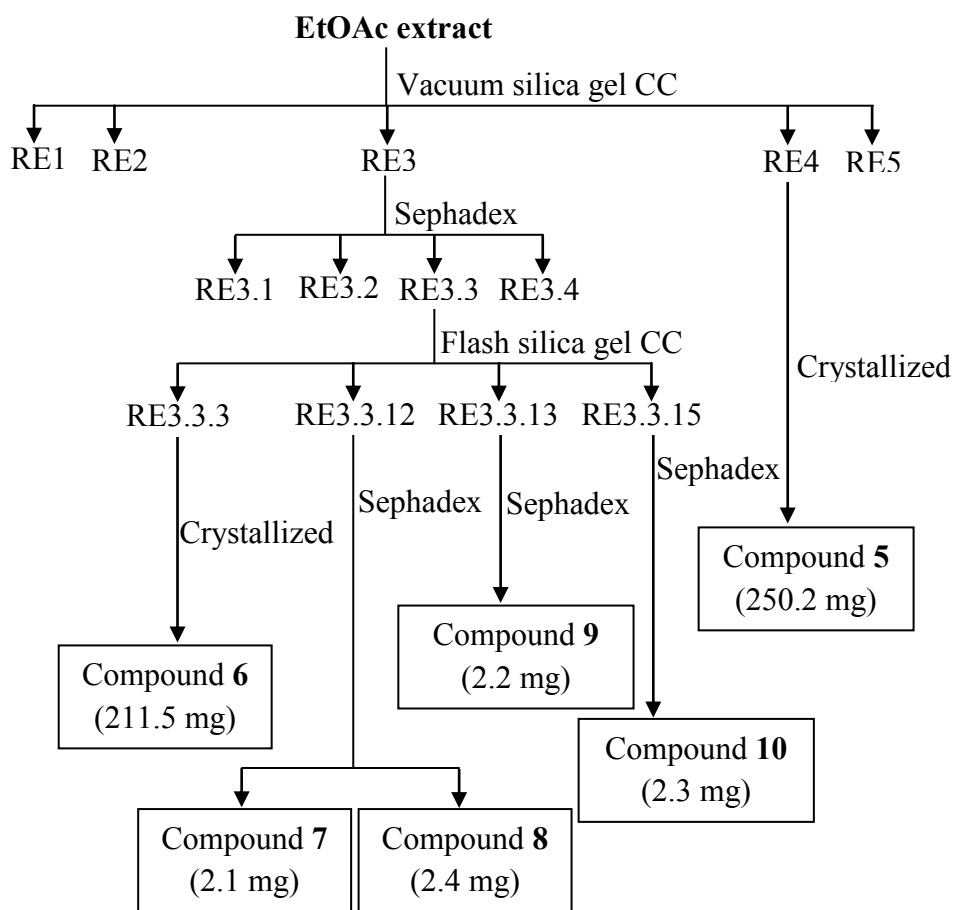
Scheme 2.5 The Isolation diagram of EtOAc extract from the roots of *C. hystrix*

2.6 Cholinesterase Inhibitory Assays

The anti-cholinesterase activities towards acetylcholinesterase (AChE) and butyrylcholinesterase (BChE) were determined using TLC-bioautography and modified microplate methods (Ellman *et al.*, 1961; Ingkaninan *et al.*, 2003). The principle of the assay was the hydrolysis of substrates acetylthiocholine (ATCI) by AChE (or BChE) to generate thiocholine and acetate. After that, thiocholine reacted with 5,5′-dithiobis(2-nitrobenzoic acid) (DTNB), or Ellman's reagent, to give yellow product, 5-thio-2-nitrobenzoate (Scheme 2.6). If natural product compounds or synthetic compounds can decrease enzyme activity or prevent the reaction between

substrate molecules and enzymes, the amount of the yellow products will be decreased.
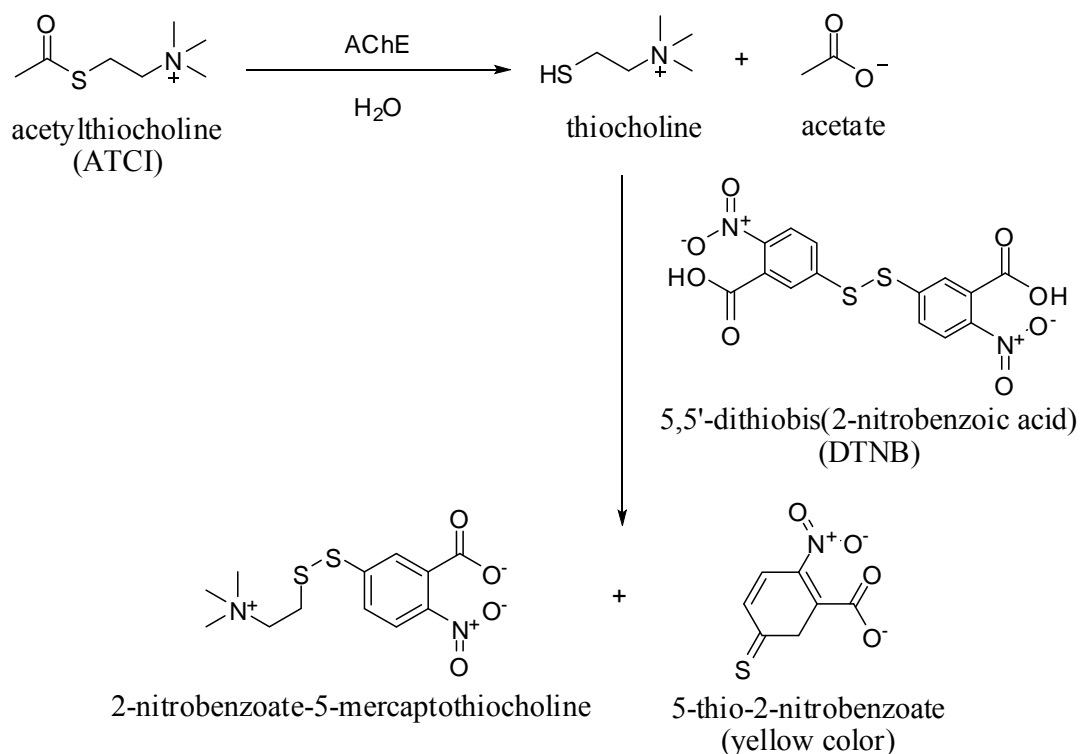
Scheme 2.5 Cholinesterase catalyzed hydrolysis of acetylthiocholine

2.6.1 Chemical Reagents

Acetylthiocholine iodide (ATCI), butyrylthiocholine iodide (BTCI), 5,5′-dithiobis(2-nitrobenzoic acid) (DTNB), acetylcholinesterase (AChE) from electric eel (Type-VI-Slypophilized powder, EC 3.1.1.7), butyrylcholinesterase (BChE) from equine serum (lypophilized powder, EC 3.1.1.8) and eserine as a standard compound were purchased from Sigma-Aldrich Co., Ltd. (St. Louis, MO, USA). Albumin from bovine serum (BSA) and *Tris*-(hydroxymethyl)-aminomethane (*Tris*-HCl) were purchased from Fluka chemical company and from Merck (Darmstadt, Germany), respectively. All solvents were distilled prior to use.

2.6.2 Chemical Preparation (Rhee *et al.*, 2001)

Buffers The following buffers are used.

Buffer A: 50 mM *Tris*-HCl (pH 8).

Buffer B: 50 mM *Tris*-HCl (pH 8) containing 0.1% BSA.

Buffer C: 50 mM *Tris*-HCl (pH 8) containing 0.1 M NaCl and 0.02 M MgCl$_2$·6H$_2$O.

The preparation of enzymes (AChE and BChE), substrates (ATCI and BTCI), and Ellman's reagent (DTNB) is described in Table 2.1.

Table 2.1 The preparation of enzymes, substrates, and Ellman's reagent

Reagents	Assays	Concentration	Solvent
Enzymes*	TLC	3 U/mL	Buffer A
	Microplate	1 U/mL	Buffer B
Substrates	TLC	5 mM	Buffer A
	Microplate	1.5 mM	Milli Q water
DTNB	TLC	5 mM	Buffer A
	Microplate	3 mM	Buffer C

Prepared from the stock solution (113 U/mL) in buffer A

2.6.3 TLC-autobiographic Method

The TLC-autobiography assay was applied to assess the preliminary anti-cholinesterase activity of *C. hystrix* extracts from leaves and roots. Each sample was dissolved in methanol to get a concentration of 10 mg/mL. Then, 10 μL of sample was spotted on a silica gel TLC plate and this plate was further developed in an appropriate solvent (chloroform:MeOH (9:1 v/v) or hexane:EtOAc (1:1, v/v)). The developed plate was dried at room temperature for at least 3 hrs and then was sprayed with a mixture of 5 mM substrate (ATCI or BTCI) and 5 mM DTNB (1:1, v/v). The plate was allowed to dry again for 5 min and sprayed with 3 U/mL cholinesterase

(AChE or BChE). After incubating the plate, white spot against yellow background revealed anti-cholinesterase activity. The yellow colour would disappear within 15 min. (Salah and Jäger, 2005)

2.5.4 Microplate Method

The extracts and isolated compounds from *C. hystrix* were tested for their anti-cholinesterase activity. The extract concentration for testing was 10 mg/mL while that of pure compounds and eserine were 1.0, 0.5, and 0.1 mg/mL. All samples were dissolved in buffer A containing not more than 10% methanol or DMSO. In the 96-well plate, 50 µL of buffer A, 25 µL of 1.5 mM substrate (ATCI or BTCI), 25 µL of sample, 125 µL of 3 mM DTNB, and 25 µL of 1.0 U/mL of enzyme (AChE or BChE) were added and absorbance was measured at a wavelength of 415 nM for 2 min at 5 sec intervals by Sunrise™ microplate reader (P-Intertrade Equipments, Australia). Each experiment was done in triplicate. The percentage of enzyme inhibition was calculated according to the equation that shown below.

$$\% \text{ inhibition} = \left(\frac{V_{blank} - V_{sample}}{V_{blank}} \right) \times 100$$

The V_{blank} is the velocity of reaction of blank without inhibitors and V_{sample} is the velocity of reaction of sample.

If the anti-cholinesterase activity of samples showed higher than 50% inhibition at a concentration of 1 mg/mL, they were further investigated for their IC_{50} values. The IC_{50} is defined as the half maximum (50%) inhibitory concentration of enzymatic activity and graphically determined from a plot of percentage inhibition versus a log final concentration from ten difference concentrations using the Graph Pad Prism 5.01 software (Graph Pad Software Inc.) (Figure 2.1).

Competition binding assays were further performed using three inhibitor concentrations; 0, IC_{50}, and $2IC_{50}$. The activities of enzymes were measured at six different substrate concentrations, in the absence and present of the inhibitor

concentration. The Lineweaver-Burk graphs were plotted using the Graph Pad Prism 5.01 software.
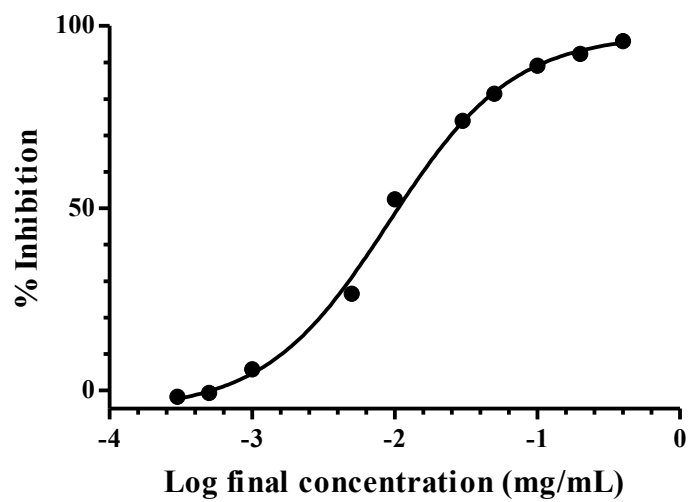
Figure 2.1 A plot of percentage inhibition versus a log final concentration values

CHAPTER III

RESULTS AND DISCUSSION

3.1 Preliminary Anti-cholinesterase Screening Test of *C. hystrix* Extracts

The *C. hystrix* leaves were extracted with MeOH and further partitioned with *n*-hexane, dichloromethane, and BuOH, respectively. After remove solvents, these extracts, which were *n*-hexane, dichloromethane, and BuOH extracts, were evaluated for their anti-AChE and BChE activities by TLC-autobiography method. The results are presented in Figure 3.1.

1 = *n*-hexane extract

2 = CH_2Cl_2 extract

3 = BuOH extract

std = eserine
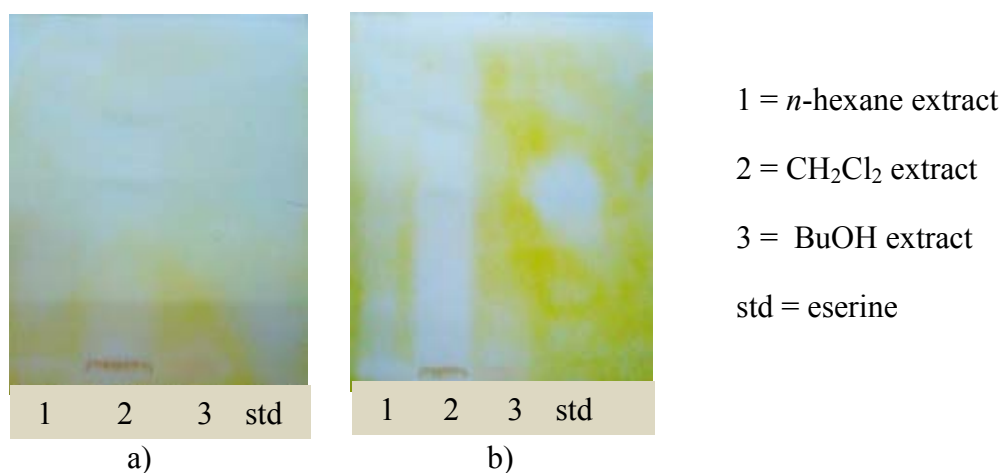
Figure 3.1 The anti-cholinesterase activities towards a) AChE and b) BChE of extracts from *C. hystrix* leaves by TLC-autobiography method

According to Figure 3.1, the inhibition zones were found in *n*-hexane and dichloromethane extracts, and less in BuOH extract towards BChE. However, only dichloromethane extract was further isolated for the active compounds because hexane extract mostly contained long chain compounds and wax. Moreover, there are no reports for the active compounds from polar extract of *C. hystrix* leaves, thus BuOH extract was also further separated.

The EtOAc extract from *C. hystrix* roots was not tested for its anti-cholinesterase activity.

3.2 Elucidation Chemical Structures of Isolated Substances from *C. hystrix* Leaves and Roots

Ten compounds (**1-10)** were obtained from the isolation of extracts of *C. hystrix* leaves and roots as described in Schemes 2.3-2.5 in Chapter II. Compounds **1-2** and **3-4** were obtained from the BuOH and dichloromethane extracts from the leaves, respectively. The EtOAc extract from the roots gave compounds **5-10**. Their chemical structures were identified based on spectroscopic data and compared with those literature values. These isolated compounds could be classified into 4 main classes which were flavanone glycosides (**1** and **2**), alkane alcohol (**3**), coumarins (**4, 6**, **7**, and **10**), limonoid (**5**), and pyranoacridone alkaloids (**8** and **9**).

3.2.1 Structural Elucidation of Compounds 1-2

Flavonoids belong to the polyphenols containing 15 carbon atoms. The flavonoids are classified into many groups, depending on their structures. Flavanones (Figure 3.2) are mostly found in many species of plants including citrus family (Rutaceae). A difference between flavanone and other flavonoids was the presence of a methylene at C-3 position which showed the proton signals at δ_H 3.04 ($J = 16.4$ and 12.8 Hz) and 2.70 ($J = 17.0$ and 3.0 Hz) in flavanone structure. Moreover, flavanones are generally glycosylated by a disaccharide at position seven to give flavanone glycosides.
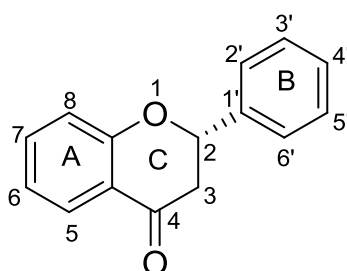
Figure 3.2 The flavanone skeleton

3.2.1.1 Hesperidin (1)

Hesperidin (1) was obtained as light yellow powders. The ^{13}C NMR spectrum of 1 (Figure A-1) displayed the presence of 28 carbon signals, comprising ten aromatic carbons (δ_C 165.0, 162.9, 162.4, 147.9, 146.3, 118.0, 114.0, 112.0, 96.4, and 95.5), eleven methine carbons (δ_C 100.4, 99.4, 78.3, 76.1, 75.4, 72.9, 72.0, 70.6, 70.2, 69.6, and 68.2) two quaternary carbons (δ_C 130.7 and 103.3) and two methylene carbons (δ_C 65.9 and 41.9), one methoxy carbon (δ_C 55.6), one carbonyl (δ_C 196.9), and one methyl carbon (δ_C 17.6). 10 aromatic carbons, 2 quaternary carbons and a carbonyl could be assigned to a flavonoid skeleton. According to flavonoid skeleton, 15 carbon signals could be found in the spectrum. The two remaining carbon signals were one from methine carbon signals which assigned for C-2 position attached to the B-ring. Another from methylene carbon signals assigned for C-3 position. Two doublet of doublet proton signals at δ_H 3.04 (J = 16.4 and 12.8 Hz) and 2.70 (J = 17.0 and 3.0 Hz) from the ^1H NMR spectrum (Figure A-2) were supported the presence of methylene carbon at C-3 position of a flavanone skeleton. The spectrum showed two aromatic proton signals at δ_H 6.85 and 6.11, both integrating for three and two proton, respectively, indicating three aromatic protons at a B-ring (H-2′, H-4′, and H-6′) and the remaining two aromatic protons at a A-ring (H-6 and H-8), respectively. The methoxy signal indicated the presence of a methoxy group at C-4′ which mostly found in the flavonoids from Rutaceae family. The remaining twelve carbon signals were assigned to a diglycoside moiety. According to the ^1H NMR spectrum, two methine proton signals at δ_H 4.85 (J = 7.2 Hz) and 4.60 (J = 0.8 Hz) were compatible with the two anomeric protons of the diglycoside moiety. Moreover, the coupling constant of those signals could be identified that this diglycoside comprised of glucose and rhamnose, respectively. The other evidences were the presence of the two-proton signal at δ_H 3.88 assigned to H-6″ of the glucose moiety and the three-proton doublet signal at δ_H 1.10 attributed to H-6‴ of the rhamnose moiety. Further comparison of ^1H and ^{13}C data of with those of published data, compound 1 was identified as hesperidin (Figure 3.3) which was previous

isolated from the fresh peel of *Citrus jambhiri* (Rutaceae) (Hamdan *et al.*, 2011). The NMR data are shown in Table 3.1.

Figure 3.3 The chemical structure of hesperidin (**1**)

3.2.1.2 Neohesperidin (2)

Neohesperidin (**2**) was obtained as light yellow powders. The ^{13}C NMR spectrum of **2** (Figure A-3) exhibited the presence of 28 carbon signals, comprising of ten aromatic carbons (δ_C 164.7, 162.8, 162.5, 148.0, 146.4, 117.9, 114.0, 112.0, 96.2, and 95.1), eleven methine carbons (δ_C 100.4, 97.4, 77.0, 76.8, 76.2, 71.8, 70.4, 70.3, 69.5, 68.3, and 68.3) two quaternary carbons (δ_C 130.8 and 103.3), and two methylene carbons (δ_C 60.0 and 42.0), including one methoxy carbon (δ_C 55.6), one carbonyl (δ_C 196.9), and one methyl carbon (δ_C 17.9). Based on the ^{1}H and ^{13}C spectrum of neohesperidin (**2**) (Figure A-4), the signals of a aglycone moiety was similar to those of hesperidin (**1**), but difference in the rhamnoglucosyl part. In ^{13}C NMR data, the signal of anomeric glucosyl carbon (δ_C 97.4) showed down-field shift than that of hesperidin (**1**) (δ_C 99.4). Moreover, in the ^{1}H NMR data, the anomeric protons (δ_H 5.16 and 5.01) and the methyl rhamnosyl proton (δ_H 1.20) showed high-field chemical shift than those of hesperidin (**1**) (δ_H 4.85 and 4.60; δ_H 1.10). These results were represented the different connectivity of glucose and rhamnose of diglycoside moiety. Previous studies were shown another diglycoside moiety, a neohesperidoside group, connected to the aglycone part (Maltese *et al.*, 2009). Moreover, above results were compatible with a neohesperidoside group that

the rhamnose ring connected to the glucose at C-2″ position. Further comparison of ^{1}H and ^{13}C data with published data, compound **2** was identified as neohesperidin (Figure 3.4) which was previous isolated from the fresh peel of *Citrus jambhiri* (Rutaceae) (Hamdan *et al.*, 2011). The NMR data are displayed in Table 3.2.
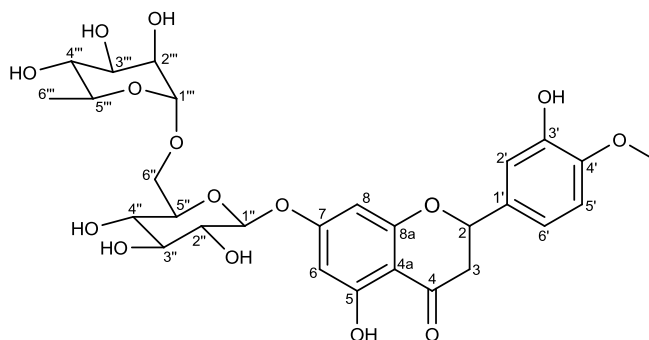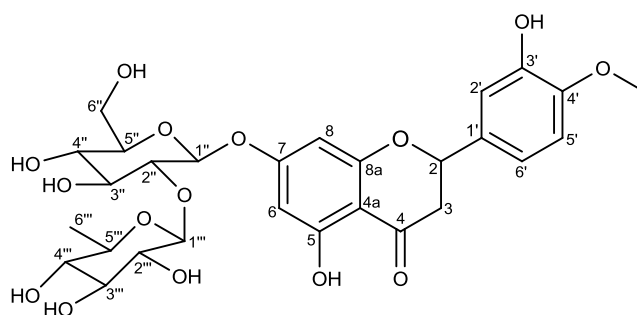

Figure 3.4 The chemical structure of neohesperidin (**2**)

Table 3.1 The ^{1}H and ^{13}C data of hesperidin (**1**) compared with those of hesperidin (Hamdan *et al.*, 2011)

Position	Hesperidin (1) (CD$_3$OD)		Hesperidin (DMSO-d_6)	
	δ_C	δ_H (int., mult., *J* in Hz)	δ_C	δ_H (int., mult., *J* in Hz)
2	78.3	5.32 (1H, *dd*, 12.0, 2.8)	79.1	5.50 (1H, *dd*, 7.6, 3.1)
3	41.9	3.04 (1H, *dd*, 16.4, 12.8)	42.7	3.20 (1H, *m*)
		2.70 (1H, *dd*, 17.0, 3.0)		2.90 (1H, *m*)
4	196.9		197.7	
4a	103.3		103.9	
5	162.9		163.5	
6	96.4	6.11 (1H, *brs*)	97.6	6.10 (1H, *d*, 2.0)
7	165.0		165.8	
8	95.5	6.11 (1H, *brs*)	96.2	6.20 (1H, *d*, 2.0)
8a	162.4		163.1	
1′	130.7		131.6	
2′	114.0	6.85 (1H, *m*)	114.8	6.90 (1H, *m*)
3′	146.3		147.1	
4′	147.9		148.6	
4′-OMe	55.6	3.78 (3H, *s*)	56.1	3.80 (3H, *s*)
5′	112.0	6.85 (1H, *m*)	112.7	6.90 (1H, *m*)
6′	118.0	6.85 (1H, *m*)	118.5	6.90 (1H, *m*)
1″	99.4	4.85 (1H, *d*, 7.2)	100.1	4.90 (1H, *d*, 7.4)
2″	70.2	3.20-3.60 (8H, *m*)	71.4	3.20-3.60 (8H, *m*)
3″	75.4	3.20-3.60 (8H, *m*)	76.1	3.20-3.60 (8H, *m*)
4″	68.2	3.20-3.60 (8H, *m*)	68.9	3.20-3.60 (8H, *m*)
5″	76.1	3.20-3.60 (8H, *m*)	76.9	3.20-3.60 (8H, *m*)
6″	65.9	3.88 (2H, *m*)	66.7	3.70 (2H, *m*)
1‴	100.4	4.60 (1H, *d*, 0.8)	101.3	4.50 (1H, *d*, 2.9)
2‴	72.0	3.20-3.60 (8H, *m*)	73.6	3.20-3.60 (8H, *m*)
3‴	69.6	3.20-3.60 (8H, *m*)	70.9	3.20-3.60 (8H, *m*)
4‴	70.6	3.20-3.60 (8H, *m*)	72.7	3.20-3.60 (8H, *m*)
5‴	72.9	3.20-3.60 (8H, *m*)	76.1	3.20-3.60 (8H, *m*)
6‴	17.6	1.10 (3H, *d*, 6.4)	18.5	1.14 (3H, *m*)

Table 3.2 The ^{1}H and ^{13}C data of neohesperidin (**2**) compared with those of neohesperidin (Hamdan *et al.*, 2011)

Position	Neohesperidin (2) (CD$_3$OD)		Neohesperidin (DMSO-d_6)	
	δ_C	δ_H (int., mult., J in Hz)	δ_C	δ_H (int., mult., J in Hz)
2	78.4	5.28 (1H, *dd*, 12.2, 2.8)	78.7	5.50 (1H, *dd*, 12.6, 3.1)
3	42.0	3.04 (1H, *dd*, 17.2, 12.4)	42.2	3.10 (1H, *m*)
		2.69 (1H, *dd*, 17.0, 3.0)		2.80 (1H, *m*)
4	196.9		197.2	
4a	103.3		100.4	
5	162.8		162.9	
6	96.2	6.06 (1H, *d*, 2.4)	96.3	6.10 (1H, *d*, 2.0)
7	164.7		164.8	
8	95.1	6.10 (1H, *d*, 2.0)	95.2	6.20 (1H, *d*, 2.0)
8a	162.5		162.7	
1′	130.8		130.8	
2′	114.0	6.86 (1H, *m*)	115.2	6.95 (1H, *d*, 2.1)
3′	146.4		146.5	
4′	148.0		147.9	
4′-OMe	55.6	3.78 (3H, *s*)	55.7	3.80 (3H, *s*)
5′	112.0	6.86 (1H, *m*)	114.2	6.92 (1H, *dd*, 2.2, 8.7)
6′	117.9	6.86 (1H, *m*)	117.9	6.90 (1H, *d*, 8.7)
1″	97.4	5.01 (1H, *d*, 7.6)	97.4	5.10 (1H, *d*, 7.4)
2″	70.3	3.20-3.60 (8H, *m*)	70.4	3.20-3.60 (8H, *m*)
3″	76.8	3.20-3.60 (8H, *m*)	76.2	3.20-3.60 (8H, *m*)
4″	68.3	3.20-3.60 (8H, *m*)	68.3	3.20-3.60 (8H, *m*)
5″	77.0	3.20-3.60 (8H, *m*)	78.4	3.20-3.60 (8H, *m*)
6″	60.0	3.84 (2H, *m*)	60.4	3.60 (2H, *m*)
1‴	100.4	5.16 (1H, *d*, 1.2)	101.3	5.18 (1H, *d*, 2.8)
2‴	71.8	3.20-3.60 (8H, *m*)	77.6	3.20-3.60 (8H, *m*)
3‴	69.5	3.20-3.60 (8H, *m*)	69.3	3.20-3.60 (8H, *m*)
4‴	70.4	3.20-3.60 (8H, *m*)	76.9	3.20-3.60 (8H, *m*)
5‴	76.2	3.20-3.60 (8H, *m*)	76.1	3.20-3.60 (8H, *m*)
6‴	17.9	1.20 (3H, *d*, 6.0)	18.0	1.20 (3H, *d*, 6.0)

3.2.2 Structural Elucidation of Alkyl Alcohol (3)

Alkyl alcohol (**3**) was obtained as white powders. The ^{1}H NMR spectrum (Figure A-6) showed the presence of three groups of proton signals; δ_H 0.88, 1.25, and 3.64. The triplet signal at δ_H 3.64 (2H, J = 6.6 Hz) and the carbon signal from the ^{13}C NMR spectrum (Figure A-5) at δ_C 63.1 were assigned to the oxygenated methylene group (C-1; -$\underline{C}$H$_2$-OH). Furthermore, the triplet signal at δ_H 0.88 (3H, J = 6.8 Hz) and the carbon signal at δ_C 14.1 were indicated the terminal methyl group. The remaining signals were attribute to many methylene groups. Further comparison of ^{1}H and ^{13}C data with published data, compound **3** was classified in alkyl alcohol displayed in Figure 3.5 (Bescetta and Gunstone, 1985; Brunel, 2007). However, this compound did not identified the exactly carbon number. The NMR data are displayed in Table 3.3.

Figure 3.5 The chemical structure of alkyl alcohol (**3**)

Table 3.3 The ^{1}H and ^{13}C data of alkyl alcohol (**3**) compared with those of 1-nonanol (Bescetta and Gunstone, 1985; Brunel, 2007)

Position	Alkyl alcohol (3) (CDCl$_3$)		1-nonanol (CDCl$_3$)	
	δ_C	δ_H (int., mult., J in Hz)	δ_C	δ_H (int., mult., J in Hz)
C-1	63.1	3.64 (2H, t, 6.6)	62.9	3.59 (2H, m)
C-2	32.8	1.25 (nH, m)	32.7	1.18-1.30 (nH, m)
C-3	25.7	1.25 (nH, m)	25.8	1.18-1.30 (nH, m)
C-n	29.6	1.25 (nH, m)	29.7	1.18-1.30 (nH, m)
-CH$_2$-	22.7	1.25 (nH, m)	22.7	1.18-1.30 (nH, m)
CH$_3$-	14.1	0.88 (3H, t, 6.8)	14.1	0.89 (3H, m)

3.2.3 Structural Elucidation of Compounds 4, 6, 7 and 10

Coumarins (Figure 3.6) are in the benzopyrone chemical class. They are found naturally in many plants especially in citrus family (Rutaceae). The characteristic signals of 1D NMR data of coumarins are a carbonyl signal at δ_C 160-180 ppm and the unsubstituted aromatic protons in the range δ_H 6.0 – 8.2 ppm. Moreover, the ^{13}C NMR exhibits two quaternary carbon signals (C-4a and C-8a). Aromatic protons in the coumarin unit are usually substituted by functional groups mostly found at C-5,-6, and -8.
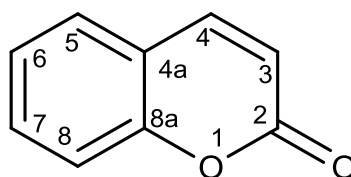
Figure 3.6 The coumarin skeleton

3.2.3.1 Oxypeucedanin Hydrate (4)

Oxypeucedanin hydrate (**4**) was obtained as white powder. The ^{13}C NMR spectrum of **4** (Figure A-7) demonstrated the presence of 16 carbon signals, comprising eight aromatic carbons (δ_C 158.1, 152.6, 148.5, 145.3, 138.9, 113.1, 104.7, and 94.8), three quaternary carbons (δ_C 114.3, 107.4, and 71.6), and two methyl carbons (δ_C 26.6 and 25.2), including one carbonyl (δ_C 161.0), one methine carbon (δ_C 76.5) and, one methylene carbon (δ_C 74.5). The ^1H NMR spectrum (Figure A-8) showed two signals at δ_H 8.17 ($J = 10.0$ Hz) and 6.29 ($J = 9.6$ Hz) as AB-type signals and *ortho*-located protons, attributable to H-4 and H-3 of the coumarin unit, respectively. The presence of singlet signal at δ_H 7.17 indicated to the aromatic proton H-8. Furthermore, the NMR spectrums showed two proton signals at δ_H 7.60 ($J = 1.2$ Hz) and 6.98 and eleven carbon signals at δ_C 161.0, 158.1, 152.6, 148.5, 104.7, 114.3, 107.4, 145.3, 138.9, 113.1, and 94.8. These data suggested the presence of the furanocoumarin skeleton (Harkar *et al.*, 1984). The remaining five carbon signals were compatible with the side-chain moiety connected to *O*-C-5 of the furanocoumarin skeleton. NMR signals of two methylene protons at δ_H 4.53 (*dd, J =*

9.6 and 2.4 Hz) and 4.44 (*dd*, *J* = 9.2 and 8.4 Hz), δ_C 74.5 (C-1′) and a doublet-of-doublet signal at δ_H 3.91 (*J* = 7.4 and 2.6 Hz), δ_C 76.5 (C-2′) with two methyl signals at δ_H 1.36 (H-4′) and 1.31 (H-5′), δ_C 26.6 (C-4′) and 25.2 (C-5′), and a quaternary carbon signal at δ_C 71.6, indicated the presence of a 2′, 3′-dihydroxy-3′, 3′-dimethylpropyl unit. Further comparison of ^{1}H and ^{13}C data with published data, compound **4** was identified as oxypeucedanin hydrate (Figure 3.7) which was previously isolated from the fresh roots of *Angelica officinalis* (Apiaceae) (Harkar *et al.*, 1984). The NMR data are displayed in Table 3.4.
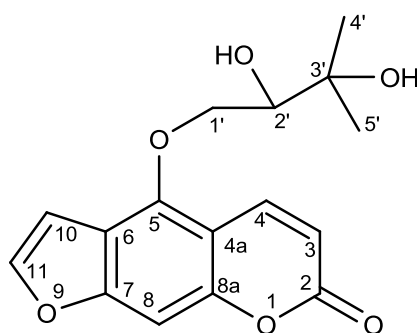

Figure 3.7 The chemical structure of oxypeucedanin hydrate (**4**)

Table 3.4 The ^{1}H and ^{13}C data of oxypeucedanin hydrate (**4**) compared with those of oxypeucedanin hydrate (Harkar *et al.*, 1984)

Position	Oxypeucedanin hydrate (4) (CDCl₃)		Oxypeucedanin hydrate (DMSO-d₆)	
	δ_C	δ_H (int., mult., J in Hz)	δ_C	δ_H (int., mult., J in Hz)
2	161.0		160.8	
3	113.1	6.29 (1H, *d*, 9.6)	111.9	6.26 (1H, *d*, 9.0)
4	138.9	8.17 (1H, *d*, 10.0)	139.7	8.13 (1H, *d*, 9.0)
4a	107.4		106.7	
5	152.6		148.9	
6	114.3		113.5	
7	158.1		157.7	
8	94.8	7.07 (1H, *s*)	93.5	7.03 (1H, *s*)
8a	148.5		145.1	
10	145.3	7.60 (1H, *d*, 1.2)	144.6	7.63 (1H, *d*, 2.2)
11	104.7	6.98 (1H, *m*)	105.0	6.96 (1H, *d*, 2.2)
1′	74.5	4.53 (1H, *dd*, 9.6, 2.4)	74.7	4.53 (2H, *m*)
		4.44 (1H, *dd*, 9.2, 8.4)		
2′	76.5	3.91 (1H, *dd*, 7.4, 2.6)	76.5	3.96 (1H, *m*)
3′	71.6		71.1	
4′	26.6	1.36 (3H, *s*)	25.1	1.33 (3H, *s*)
5′	25.2	1.31 (3H, *s*)	25.1	1.33 (3H, *s*)

3.2.3.2 Xanthyletin (6)

Xanthyletin (**6**) was obtained as colourless needles. The ^{13}C NMR spectrum of **6** (Figure A-11) demonstrated the presence of 14 carbon signals, including eight aromatic carbons (δ_C 156.8, 155.5, 143.3, 131.2, 124.8, 120.8, 113.0, and 104.4), three quaternary carbon (δ_C 118.5, 112.7, and 77.7), one carbonyl (δ_C 161.2), and two methyl carbon (δ_C 28.3 (Me×2)). The ^{1}H NMR spectrum (Figure A-12) showed 8 signals of six aromatic proton signals (δ_H 7.57, 7.04, 6.71, 6.33, 6.21, and 5.68) and two methyl proton (δ_H 1.46 (Me×2)). The spectrum exhibited two AB-type signals at δ_H 7.57 and 6.21 (both with J = 9.6 Hz) and two singlet signals at δ_H 7.04 and 6.71, indicating the presence of 6, 7,-disubstituted coumarin skeleton. Moreover, the spectrum showed two doublet signals, belonging to the aromatic

protons H-2′ and H-3′ at δ_H 5.68 and 6.33 (both with J = 10.0 Hz), respectively. Two methyl singlets were also apparent at δ_H 1.46 (6H) and correlated with the quaternary carbon at δ_C 77.7 (C-1′). In addition, the ^{13}C NMR spectrum exhibited twelve signals at δ_C 161.2, 156.8, 155.5, 143.3, 131.2, 124.8, 120.8, 113.0, 118.5, 112.7, 104.4, and 77.7. These observations suggested the presence of a cyclized prenyl group attached to C-6. Further comparison ^{1}H and ^{13}C data with published data, compound **6** was identified as xanthyletin (Figure 3.8) which was previously isolated from the roots *Citrus sinensis* (Rutaceae) (Cazal *et al.*, 2009). The NMR data are displayed in Table 3.5.
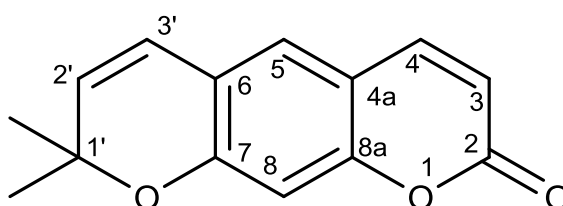

Figure 3.8 The chemical structure of xanthyletin (**6**)

Table 3.5 The ^{1}H and ^{13}C data of xanthyletin (**6**) compared with those of xanthyletin (Cazal *et al.*, 2009)

Position	Xanthyletin (6) (CDCl$_3$)		Xanthyletin (CDCl$_3$)	
	δ_C	δ_H (int., mult., J in Hz)	δ_C	δ_H (int., mult., J in Hz)
2	161.2		161.1	
3	104.4	6.21 (1H, *d*, 9.6)	104.3	6.24 (1H, *d*, 9.2)
4	143.3	7.57 (1H, *d*, 9.6)	143.3	7.60 (1H, *d*, 9.2)
4a	112.7		112.7	
5	131.2	7.04 (1H, *s*)	131.2	7.04 (1H, *s*)
6	118.5		118.5	
7	156.8		156.8	
8	113.0	6.71 (1H, *s*)	112.9	6.72 (1H, *s*)
8a	155.5		155.4	
1′	77.7		77.7	
2′	124.8	5.68 (1H, *d*, 10.0)	124.7	5.71 (1H, *d*, 9.6)
3′	120.8	6.33 (1H, *d*, 10.0)	120.7	6.36 (1H, *d*, 9.6)
1′-Me	28.3	1.46 (6H, *s*)	28.3	1.43 (6H, *s*)

3.2.3.3 Crenulatin (7)

Crenulatin (7) was obtained as yellow powders. The ^{13}C NMR spectrum of 7 (Figure A-13) displayed the presence of 11 carbon signals, comprising two quaternary carbons (δ_C 120.8 and 113.8), two carbonyls (δ_C 18.7. and 167.1), six aromatic carbons (δ_C 159.6 (2C), 143.2, 129.0, 114.6, and 99.9), and one methoxy carbon (δ_C 56.4). The ^{1}H NMR spectrum (Figure A-14) showed two AB-type signals at δ_H 7.62 and 6.26 (both with J = 9.6 Hz) and two singlet signals at δ_H 7.93 and 6.81, indicating the presence of 6, 7,-disubstituted coumarin skeleton. According to the nine carbon signals at δ_C 167.2, 159.6 (2C), 143.2, 129.0, 120.8, 114.6, 113.8, and 99.9, these data suggested the presence of coumarin unit. The carbonyl at δ_C 187.7 and δ_H 10.35 were assigned as the aldehyde part at C-6 position and the methoxyl carbon at δ_C 56.4 and δ_H 3.94 were assigned to the methoxy group at C-7 position. Further comparison ^{1}H and ^{13}C data with published data, compound 7 was identified as crenulatin (Figure 3.9) which was previously isolated from the root barks of *Hesperathusa crenulate* (Rutaceae) and *Citrus sinensis* (Rutaceae) (Basa and Tripathy, 1982; Wu and Furukawa, 1983). The NMR data are displayed in Table 3.6.
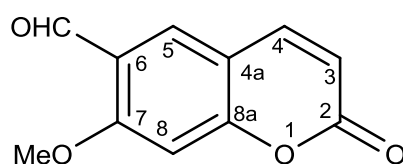

Figure 3.9 The chemical structure of crenulatin (7)

Table 3.6 The ^{1}H and ^{13}C data of crenulatin (**7**) compared with those of crenulatin (Basa and Tripathy, 1982; Wu and Furukawa, 1983)

Position	Compound 7 (CDCl$_3$)		Crenulatin (CDCl$_3$)	
	δ_C	δ_H (int., mult., J in Hz)	δ_C	δ_H (int., mult., J in Hz)
2	167.1		164.2	
3	114.6	6.26 (1H, d, 9.6)	114.5	6.26 (1H, d, 10.0)
4	143.2	7.62 (1H, d, 9.6)	143.2	7.63 (1H, d, 10.0)
4a	113.8		113.8	
5	129.0	7.93 (1H, s)	128.9	7.91 (1H, s)
6	120.8		122.1	
7	159.6		159.7	
8	99.9	6.81 (1H, s)	100.0	6.83 (1H, s)
8a	159.6		159.5	
7-OMe	56.4	3.94 (3H, s)	55.8	3.97 (3H, s)
6-CHO	187.7	10.35 (1H, s)	187.7	10.33 (1H, s)

3.2.3.4 Umbelliferone (10)

Umbelliferone (**10**) was obtained as white needles. The ^{13}C NMR spectrum of **10** (Figure A-19) displayed the presence of 9 carbon signals, comprising seven aromatic carbons (δ_C 162.2, 154.3, 144.7, 130.4, 113.8, 112.9, and 103.3), including one carbonyl (δ_C 157.1), and one quaternary carbon (δ_C 112.9). The ^{1}H NMR spectrum (Figure A-20) showed two doublet signals δ_H 7.86 and 6.16 (both with J = 9.6 Hz) as AB-type signals and *ortho*-located protons, compatible to H-4 and H-3 of the coumarin unit, respectively. The doublet-of-doublet signal at δ_H 6.84 (J = 2.2 and 8.2 Hz) revealed the one *ortho*-located and one *meta*-located protons, which is characteristic of a 7-substituted coumarin skeleton (Kong *et al.*, 1996). Further comparison ^{1}H and ^{13}C data with published data, compound **10** was identified as umbelliferone (Figure 3.10) which was previously isolated from the roots of *Peucedanum praeruptorum* (Apiaceae) (Kong *et al.*, 1996). The NMR data are displayed in Table 3.7.
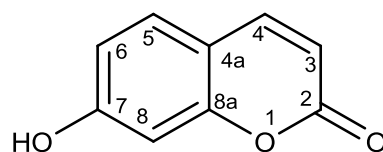
Figure 3.10 The chemical structure of umbelliferone (**10**)

Table 3.7 The ^{1}H and ^{13}C data of umbelliferone (**10**) compared with those of umbelliferone (Kong *et al.*, 1996)

Position	Umbelliferone (10) (acetone-d_6)		Umbelliferone (DMSO)	
	δ_C	δ_H (int., mult., J in Hz)	δ_C	δ_H (int., mult., J in Hz)
2	167.1		164.2	
3	112.9	6.16 (1H, *d*, 9.6)	112.2	6.10 (1H, *d*, 9.5)
4	144.7	7.86 (1H, *d*, 9.6)	144.4	7.79 (1H, *d*, 9.5)
4a	113.8		113.8	
5	130.4	7.51 (1H, *d*, 8.8)	129.7	7.42 (1H, *d*, 8.4)
6	113.8	6.84 (1H, *dd*, 2.2, 8.2)	113.4	6.77 (1H, *dd*, 2.2, 8.4)
7	162.2		162.0	
8	103.3	6.75 (1H, *d*, 1.6)	102.8	6.71 (1H, *d*, 2.2)
8a	154.3		156.3	

3.2.4 Structural Elucidation of Limonin (5)

Limonin (**5**) was obtained as white powder. The ^{13}C NMR spectrum of **5** (Figure A-9) displayed the presence of 26 signals, comprising three carbonyl carbons (δ_C 206.0, 169.0, and 166.6), three olefinic carbons (δ_C 143.2, 141.1, and 109.6), six quaternary carbons (δ_C 120.0, 80.3, 65.7, 51.3, 46.0, and 38.0), five methine carbons (δ_C 79.1, 77.8, 60.5, 53.9, and 48.1), two methane carbons (δ_C 60.5 and 48.1), five methylene carbon (δ_C 65.3, 36.4, 35.6, 30.2, and 18.9), and four methyl carbons (δ_C 30.8, 21.4, 20.7, and 17.6). The ^{1}H NMR spectrum (Figure A-10) demonstrated three olefinic protons (δ_H 7.40, 7.39, and 6.33), five methine protons (δ_H 5.46, 4.02 (2H), 2.54, and 2.22), eight methylene protons (δ_H 4.75, 4.45, 2.96, 2.67, 2.85, 2.45, 1.80, and 1.50), and four methyl protons (δ_H 1.28, 1.17 (Me×2), and 1.06). The proton signals showed characteristic of a furan ring signal, where H-21 and H-23

appeared as multiplets at δ_H 7.40 and 7.39, respectively. The furan hydrogen H-22 showed as broad singlet at δ_H 6.33. The hydrogen H-17, from the epoxylactone ring was observed at δ_H 5.46 (*s*, 1H). Two carbonyl signals at δ_C 169.0 and 166.6 indicated the presence of two lactone rings. The remaining signal at δ_C 206.0 was assigned to the ketone group in cyclohexane ring. The presence of two doublet signals at δ_H 4.75 (1H, *J* = 12.8 Hz) and 4.45 (1H, *J* = 13.2 Hz) indicated to the geminal hydrogens at C-19. Moreover, a pair of signals at δ_H 2.96 (1H, *dd*, *J* = 16.8 and 3.6 Hz) and 2.67 (1H, *d*, *J* = 16.8 Hz) indicated to the geminal hydrogens at C-2. The other pair of doublet-of-doublet signals at δ_H 2.85 (1H, *J* = 15.2 and 15.2 Hz) and 2.45 (1H, *J* = 14.4 and 2.8 Hz) also indicated to the geminal hydrogens at C-6. The spectrum exhibited the signals at δ_H 1.81 and 1.50 (both with 2H, *m*) indicating the presence of two methylene group in the cyclohexane ring. Four singlet signals at δ_H 1.28, 1.17 (Me×2) and 1.06 were attributed to four methyl groups C-25, C-24, C-18, and C-30, respectively. The carbon signals at δ_C 30.8, 21.4, 20.7 and 17.6 also supported these conclusions. Further comparison ^{1}H and ^{13}C data with published data, compound **5** was identified as limonin (Figure 3.11) which was previously isolated from the barks of *Phellodendron amurense* (Rutaceae) (Min *et al.*, 2007). The NMR data are displayed in Table 3.8.
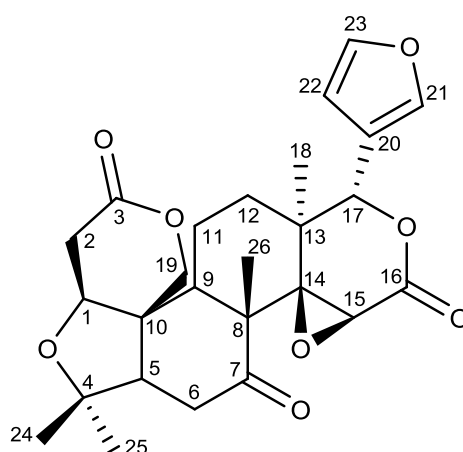
Figure 3.11 The chemical structure of limonin (**5**)

Table 3.8 The ^{1}H and ^{13}C data of limonin (**5**) compared with those of limonin (Min *et al.*, 2007)

Position	Limonin (5) (CDCl₃)		Limonin (CDCl₃)	
	δ_C	δ_H (int., mult., *J* in Hz)	δ_C	δ_H (int., mult., *J* in Hz)
1	79.1	4.02 (1H, *brs*)	79.1	4.04 (1H, *brs*)
2	35.6	2.96 (1H, *dd*, 16.8, 3.6)	35.6	2.98 (1H, *dd*, 16.7, 1.8)
		2.67 (1H, *d*, 16.8)		2.68 (1H, *dd*, 16.7, 1.8)
3	169.0		169.0	
4	80.3		80.3	
5	60.5	2.22 (1H, *dd*, 15.6, 2.8)	60.5	2.23 (1H, *dd*, 15.8, 3.2)
6	36.4	2.85 (1H, *dd*, 15.2, 15.2)	36.4	2.85 (1H, *dd*, 15.8, 14.4)
		2.45 (1H, *dd*, 14.4, 2.8)		2.47 (1H, *dd*, 14.4, 3.2)
7	206.1		206.0	
8	51.3		51.3	
9	48.1	2.54 (1H, *dd*, 12.4, 2.4)	48.1	2.56 (1H, *dd*, 12.2, 2.9)
10	46.0		45.9	
11	18.9	1.80 (2H, *m*)	18.9	1.81 (2H, *m*)
12	30.2	1.50 (2H, *m*)	30.1	1.50 (2H, *m*)
13	38.0		37.9	
14	65.7		65.7	
15	53.9	4.02 (1H, *brs*)	53.8	4.04 (1H, *brs*)
16	166.6		166.6	
17	77.8	5.46 (1H, *s*)	77.8	5.47 (1H, *s*)
18	21.4	1.17 (3H, *s*)	21.4	1.17 (3H, *s*)
19	65.3	4.75 (1H, *d*, 12.8)	65.3	4.76 (1H, *d*, 13.2)
		4.45 (1H, *d*, 13.2)		4.46 (1H, *d*, 13.2)
20	120.0		120.0	
21	141.1	7.40 (1H, *m*)	141.1	7.41 (1H, *m*)
22	109.6	6.33 (1H, *brs*)	109.6	6.34 (1H, *m*)
23	143.2	7.39 (1H, *m*)	143.2	7.40 (1H, *m*)
24	20.7	1.17 (3H, *s*)	20.7	1.18 (3H, *s*)
25	30.8	1.28 (3H, *s*)	30.8	1.29 (3H, *s*)
26	17.6	1.06 (3H, *s*)	17.6	1.07 (3H, *s*)

3.2.5 Structural Elucidation of Compounds 8 and 9

Pyranoacridone alkaloids are in alkaloid family that is found in some Rutaceae species. The pyranoacridone alkaloids (Figure 3.12) based on the acridine skeleton, with a carbonyl group at 9-position. Apart from the carbonyl carbon signal at δ_C 160-180, mostly acridone skeletons which are found in Rutaceae family would be attached with *N*-methyl group. The carbonyl signals bearing a hydrogen bond of 1-hydroxy group are observed in the region 180-190 ppm. The C-1′ and C-2′ are affected by the *N*-methyl group, so the signals appear at 120-125 ppm. Moreover, the *N*-methyl signal is observed at 47-50 ppm (Furakawa *et al.*, 1983).
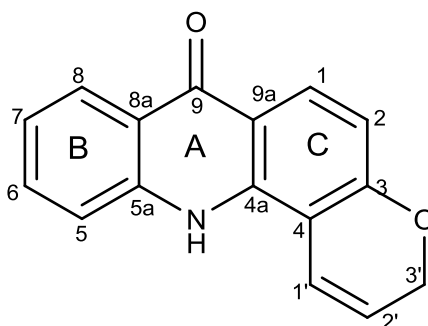
Figure 3.12 The pyranoacridone skeleton

3.2.5.1 5-hydroxynoracronycine (8)

5-hydroxynoracronycine (**8**) was obtained as red powders. The ^{13}C NMR spectrum of **8** (Figure A-15) showed the presence of 19 carbon signals, comprising eleven aromatic carbons (δ_C 149.3, 162.2, 165.6, 148.9, 138.1, 121.7, 120.9, 124.2, 124.8, 117.3, and 98.2), four quaternary carbons (δ_C 124.9, 106.7 (C×2), and 77.5), two methyl carbons (δ_C 27.3 (C×2)), one carbonyl (δ_C 180.7), and one methylamine carbon (δ_C 49.1). The ^1H NMR spectrum (Figure A-16) displayed an ABC pattern of signals at δ_H 7.32 (1H, *d*, *J* = 7.2 Hz), 7.22 (1H, *t*, *J* = 7.8 Hz), and 7.81 (1H, *dd*, *J* = 1.2 and 8.0 Hz) due to H-6, -7, and -8, respectively. The AB-type signals at δ_H 6.76 (1H, *d*, *J* = 9.6 Hz) and 5.69 (1H, *d*, *J* = 10.0 Hz) and two singlet siganls at δ_H 1.51 (6H) revealed the presence of a dimethylpyran system attached to

ring C. The singlet at δ_H 3.85 was assigned to *N*-methyl group. The ^{13}C NMR spectrum also supported these conclusions, and signals of *N*-methyl carbon and the aromatic C-1′ of the dimethylpyran ring appeared at δ_C 49.1 and 121.7, respectively. Further comparison ^{1}H and ^{13}C data with published data, compound **8** was identified as 5-hydroxynoracronycine (Figure 3.13) which was previously isolated from the roots of *Citrus depressa* (Rutaceae) (Wu *et al.*, 1983; Furukawa *et al.*, 1983). The NMR data are displayed in Table 3.9.
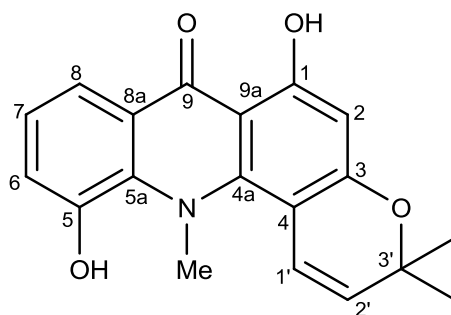
Figure 3.13 The chemical structure of 5-hydroxynoracronycine (**8**)

Table 3.9 The ^{1}H and ^{13}C data of 5-hydroxynoracronycine (**8**) compared with those of 5-hydroxynoracronycine (Wu *et al.*, 1983; Furukawa *et al.*, 1983)

Position	5-hydroxynoracronycine (9) (acetone-d_6)		5-hydroxynoracronycine (Acetone-d_6)	
	δ_C	δ_H (int., mult., *J* in Hz)	δ_C	δ_H (int., mult., *J* in Hz)
1	162.2		161.1	
2	98.2	6.12 (1H, *s*)	97.5	6.18 (1H, *s*)
3	165.6		164.3	
4	106.7		106.9	
4a	149.3		148.5	
N-Me	49.1	3.85 (3H, *s*)	48.6	3.87 (3H, *s*)
5a	138.1		137.0	
5	148.9		147.7	
6	120.9	7.32 (1H, *d*, 7.2)	120.1	7.40 (1H, *dd*, 2.0, 7.0)
7	124.2	7.22 (1H, *t*, 7.8)	123.3	7.25 (1H, *t*, 7.0)
8	117.3	7.81 (1H, *dd*, 1.2, 8.0)	116.0	7.88 (1H, *dd*, 2.0, 7.0)
8a	124.9		124.7	
9	180.7		181.8	
9a	106.7		102.1	
1′	121.7	6.76 (1H, *d*, 9.6)	121.0	6.81 (1H, *d*, 10.0)
2′	124.8	5.69 (1H, *d*, 10.0)	123.6	5.73 (1H, *d*, 10.0)
3′	77.5		76.6	
3′-Me	27.3	1.51 (6H, *s*)	27.1	1.51 (6H, *s*)

3.2.5.1 Citracridone-I 9

Citracridone-I **9** was obtained as red powders. The ^{13}C NMR spectrum of **9** (Figure A-17) demonstrated the presence of 20 carbon signals, comprising eleven aromatic carbons (δ_C 164.4, 164.7, 158.3, 154.3, 153.2, 143.5, 124.7, 123.5, 120.4, 111.9, and 98.7), four quaternary carbons (δ_C 116.4, 108.1, 103.9, and 77.2), two methyl carbons (δ_C 29.7 and 27.3), one carbonyl (δ_C 187.1), one methoxy carbon (δ_C 60.0), and one methylamine carbon (δ_C 49.1). The AB-type signals at δ_H 6.92 (1H, *d*, *J* = 8.8 Hz) and 7.99 (1H, *d*, *J* = 8.8 Hz) in The ^{1}H NMR spectrum (Figure A-18) were assigned to *ortho*-located protons at H-7 and -8, respectively. Another AB-type at δ_H 6.47 (1H, *d*, *J* = 10.0 Hz) and 5.51 (1H, *d*, *J* = 9.6

Hz) and a six-proton singlet at δ_H 1.45 suggested the presence of a dimethylpyran unit attached to ring C. Two singlets at δ_H 3.63 and 3.84 (each 3H) were attributed to a *N*-methyl group and a methoxy group. The carbon signals of the *N*-methyl carbon and the aromatic C-1′ of a dimethylpyran ring appeared at δ_C 49.1 and 121.7, supported these conclusions. Further comparison ^{1}H and ^{13}C data with published data, compound **9** was identified as citracridone-I (Figure 3.14) which was previously isolated from the roots of *Citrus depressa* (Rutaceae) (Wu *et al.*, 1983; Furukawa *et al.*, 1983). The NMR data are displayed in Table 3.10.
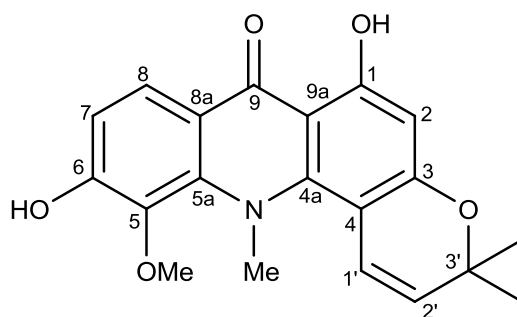
Figure 3.14 The chemical structure of citracridone-I (**9**)

Table 3.10 The ^{1}H and ^{13}C data of citracridone-I (**9**) compared with those of

citracridone-I (Wu *et al.*, 1983; Furukawa *et al.*, 1983)

Position	Citracridone-I (9) (CDCl$_3$)		Citracridone-I (CDCl$_3$ + DMSO-d_6)	
	δ_C	δ_H (int., mult., *J* in Hz)	δ_C	δ_H (int., mult., *J* in Hz)
1	164.4		162.9	
2	98.7	6.29 (1H, *s*)	97.5	6.23 (1H, *s*)
3	164.7		164.2	
4	103.9		102.9	
4a	154.3		147.1	
N-Me	47.8	3.63 (3H, *s*)	49.7	3.75 (3H, *s*)
5a	143.5		134.6	
5	153.2		140.5	
5-OMe	60.0	3.84 (3H, *s*)	60.5	3.91 (3H, *s*)
6	158.3		155.7	
7	111.9	6.92 (1H, *d*, 8.8)	113.1	7.00 (1H, *d*, 9.0)
8	123.5	7.99 (1H, *d*, 8.8)	122.5	8.01 (1H, *d*, 9.0)
8a	116.4		117.6	
9	187.1		180.3	
9a	108.1		105.2	
1′	120.4	6.47 (1H, *d*, 10.0)	121.4	6.63 (1H, *dd*, 1.0, 10.0)
2′	124.7	5.51 (1H, *d*, 9.6)	123.6	5.61 (1H, *d*, 10.0)
3′	77.2		85.2	
3′-Me	29.7	1.45 (6H, *s*)	28.2	1.53 (6H, *s*)
	27.2			
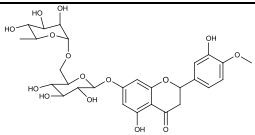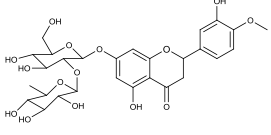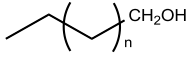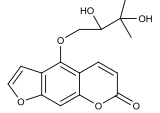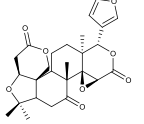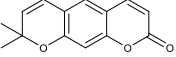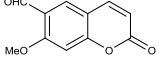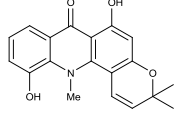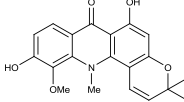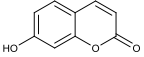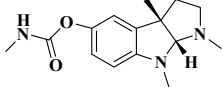
3.3 Cholinesterase Inhibitory Activities of Isolated Substances from *C. hystrix* Leaves and Roots

All isolated compounds (compounds **1-10**) were further determined their anti-cholinesterase activities by the colorimetric method. Eserine was used as a positive control.

The AChE and BChE inhibition percentages of all isolated substances, at the final concentration 0.5, 0.1 and 0.05 mg/mL, are displayed in Tables 3.11 and 3.12, respectively. All isolated substances showed dose-dependent manner as shown in Figures 3.15-3.24. Nevertheless, they showed low-to-moderate activities (<50%

inhibition percentages), except neohesperidin (**2**) towards AChE, and oxypeucedanin hydrate (**4**) and xanthyletin (**6**) towards both AChE and BChE, compared to eserine. According to less solubility of substances under assay condition and low amount of some isolated substances, only neohesperidin (**2**), oxypeucedanin hydrate (**4**) and xanthyletin (**6**) were further evaluated for their IC_{50} values. The IC_{50} value of neohesperidin (**2**) towards AChE was 160.1 μM, and that of oxypeucedanin hydrate (**4**) were 570.3 and 260.8 μM toward AChE and BChE, respectively, by the Prism Software calculation. These values were quite high comparing with those of eserine which were 0.73 and 2.54 μM of AChE and BChE, respectively. The IC_{50} values of xanthyletin (**6**) were 116.2 μM and 37.4 μM toward AChE and BChE, respectively. The IC_{50} value of xanthyletin (**6**) towards BChE was 14-folds higher than that of eserine. The dose response curves of xanthyletin (**6**) and eserine towards BChE are displayed in Figure 3.25. Neohesperidin (**2**) showed the AChE inhibition in the agreement with the previous studies. The previous studies revealed that the structure of flavonoids for the AChE inhibition required the presence of 4′-methoxyl group, and 7-O-sugar moiety as well as the length and the interglycosidic linkage of sugar chain (Lim *et al.*, 2007; Fan *et al.*, 2008; Khan *et al.*, 2009). Oxypeucedanin hydrate (**4**) and xanthyletin (**6**) were coumarin fused with furan and pyran at C-6 position, respectively. Moreover, oxypeucedanin hydrate (**4**) showed the presence of free hydroxyl group at C-3′ position. These results supported the finding of previous studies that the coumarin skeleton containing a pyrone moiety, and a free hydroxyl group at C-3′ position was crucial for the inhibitory activity (Kang *et al.*, 2001; Youkwan *et al.*, 2010; Wszelaki *et al.*, 2011). According to the structures of enzymes, AChE has a characteristic narrow gorge leading to its active site, while the gorge of BChE is wider (Darvesh *et al.*, 2003). The coumarins with a longer and more side chain are not able to pass the narrow gorge of AChE's active site, but able in BChE's gorge, thus, they would be more selective towards BChE. Moreover, this study is the first report of butyrylcholinesterase inhibitory activity of xanthyletin. So, the results suggested that xanthyletin might be the promising candidate for the development, and further investigation to be an effective drug for the treatment of AD.
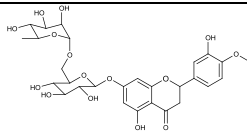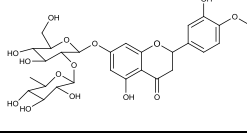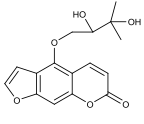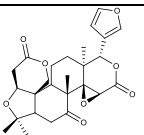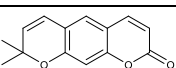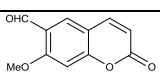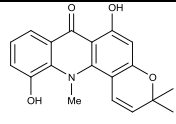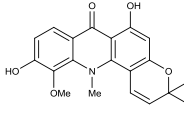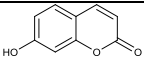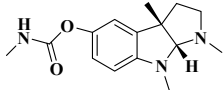
Table 3.11 The AChE inhibitory activity of all isolated substances from the leaves
and roots of *C. hystrix* at final concentrations of 0.5, 0.1, and 0.05 mg/mL

Substance	Structure	% AChE Inhibition[a] at the final concentrations of (mg/mL)		
		0.5	0.1	0.05
1		59.21	30.37	8.65
2		70.00	48.58	38.74
3		26.74	22.71	12.45
4		58.47	39.41	34.19
5		20.57	18.26	0
6		77.89	70.62	66.93
7		35.69	29.88	6.18
8		29.48	25.50	23.41
9		42.63	32.47	20.72
10		30.38	27.29	25.76
Eserine[b]		99.98	99.93	99.86

[a]*Results are expressed as means (n = 2)*

[b]*Positive control*

Table 3.12 The BChE inhibitory activity of all isolated substances from the leaves and roots of *C. hystrix* at final concentrations of 0.5, 0.1, and 0.05 mg/mL

Substance	Structure	% BChE Inhibition[a] at the final concentrations of (mg/mL)		
		0.5	0.1	0.05
1		28.43	2.25	0
2		13.51	10.58	4.99
3		16.39	11.54	11.44
4		62.47	49.80	27.03
5		18.11	0.47	0
6		92.45	79.29	58.29
7		36.99	26.15	20.99
8		53.92	41.69	35.77
9		83.91	71.68	68.39
10		42.32	14.95	9.24
Eserine[b]		99.56	98.55	98.12

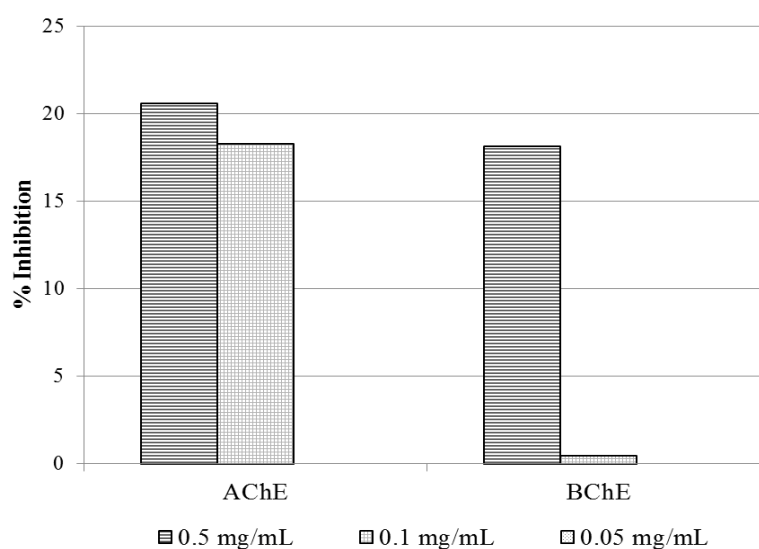[a]*Results are expressed as means (n = 2)*

[b]*Positive control*
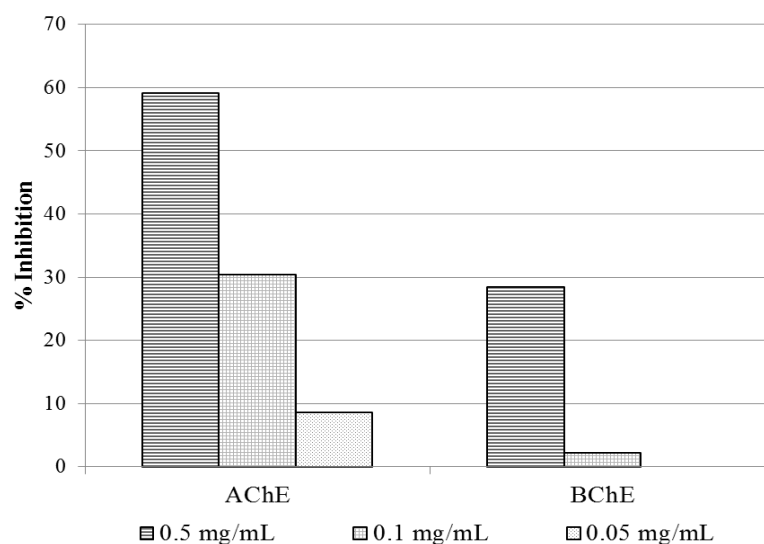
Figure 3.15 The cholinesterase inhibitory activities of hesperidin (**1**) at the final concentrations of 0.5, 0.1, and 0.05 mg/mL. Data are express as means ($n = 2$)
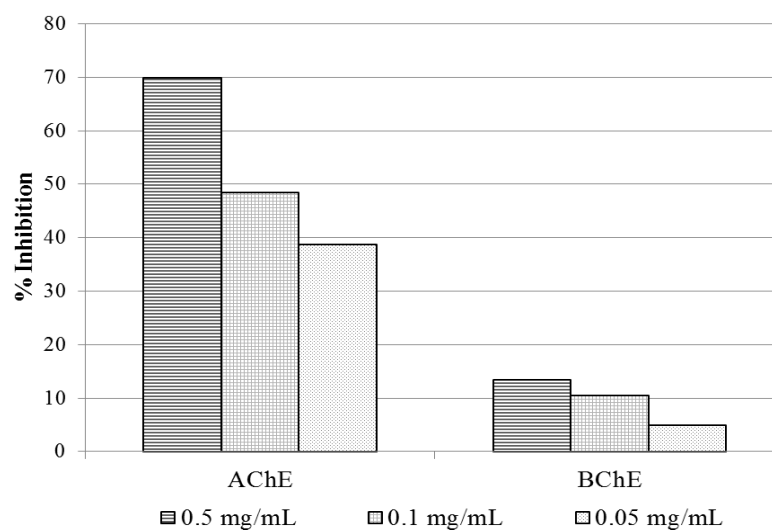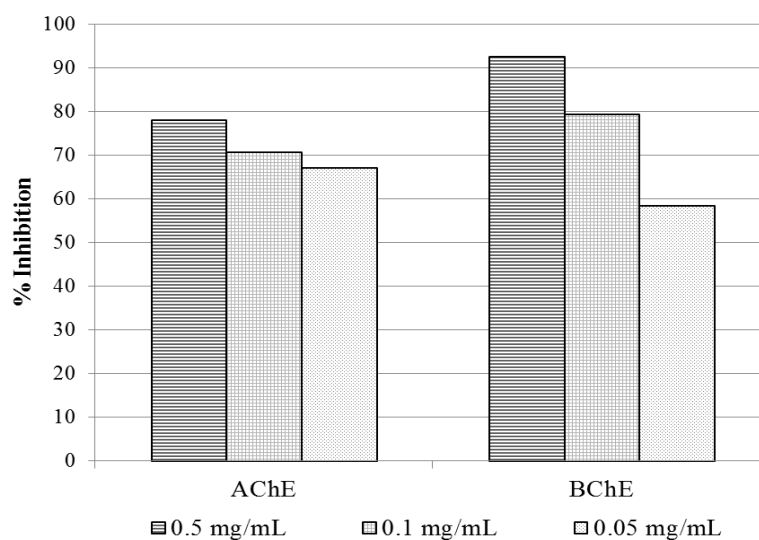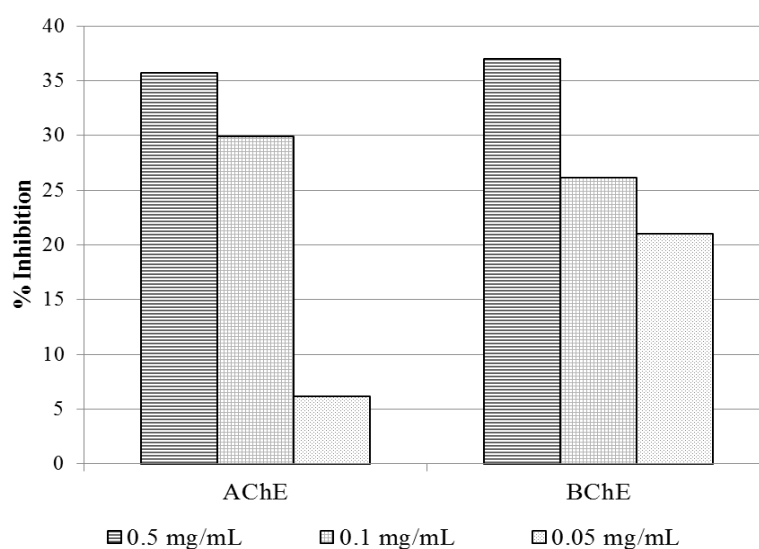

Figure 3.16 The cholinesterase inhibitory activities of neohesperidin (**2**) at the final concentrations of 0.5, 0.1, and 0.05 mg/mL. Data are express as means ($n = 2$)
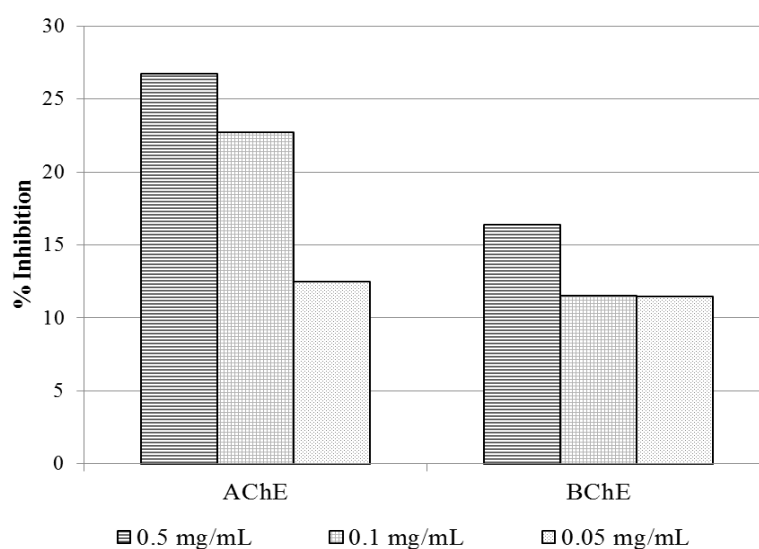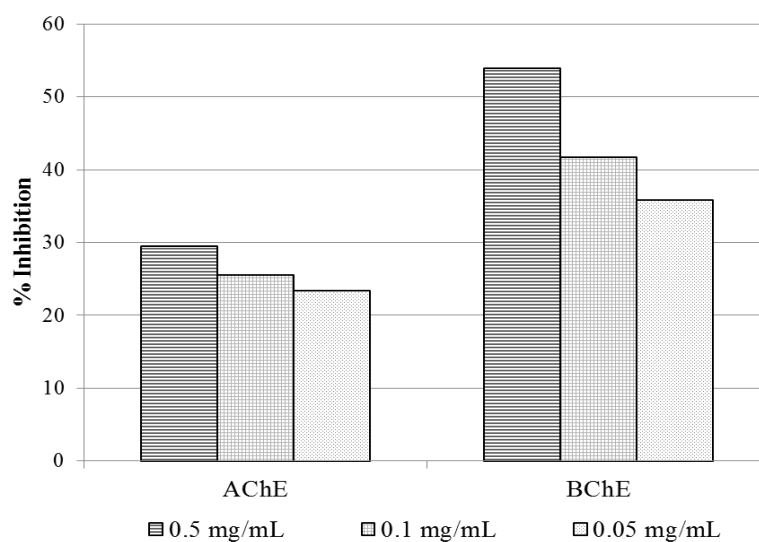
Figure 3.17 The cholinesterase inhibitory activities of alkyl alcohol (**3**) at the final concentrations of 0.5, 0.1, and 0.05 mg/mL. Data are express as means (*n* = 2)
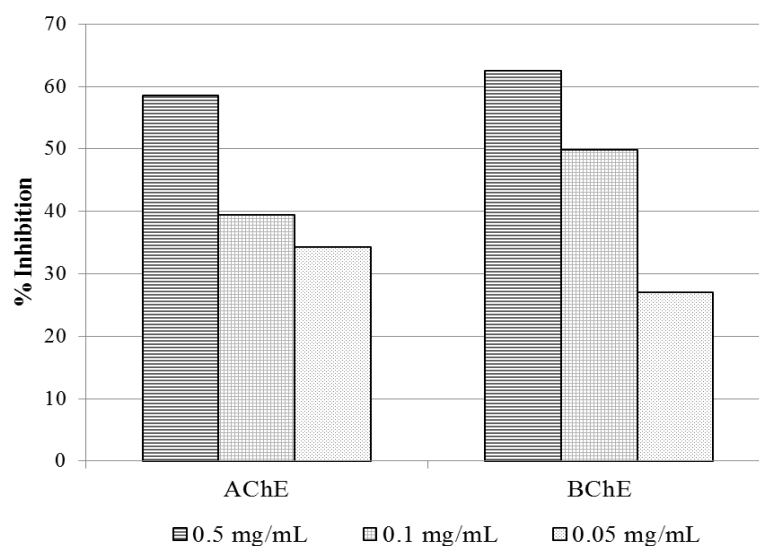
Figure 3.18 The cholinesterase inhibitory activities of oxypeucedanin hydrate (**4**) at the final concentrations of 0.5, 0.1, and 0.05 mg/mL. Data are express as means (*n* = 2)

Figure 3.19 The cholinesterase inhibitory activities of limonin (**5**) at the final concentrations of 0.5, 0.1, and 0.05 mg/mL. Data are express as means ($n = 2$)
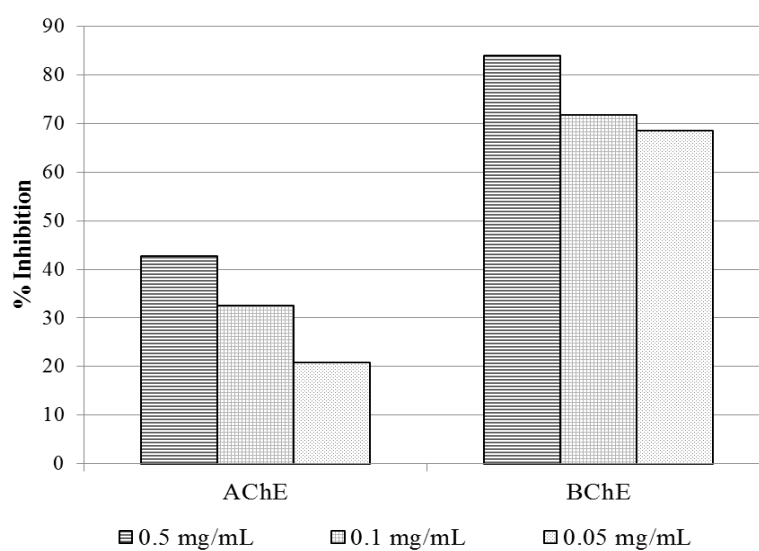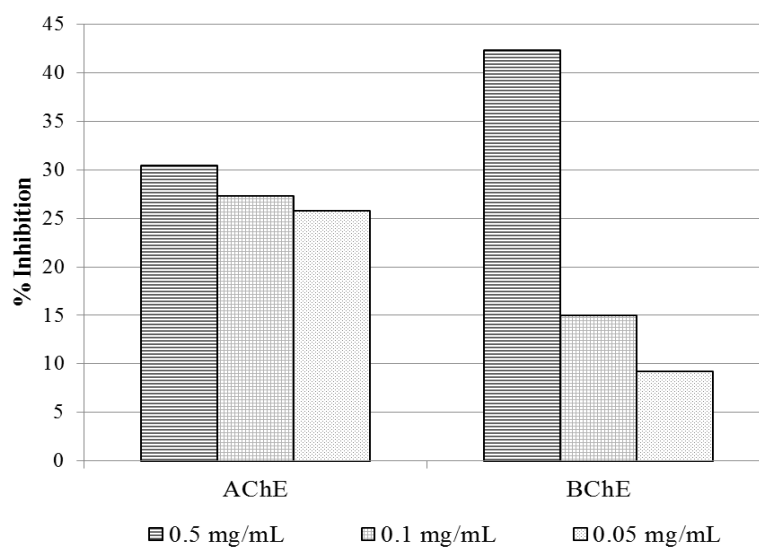

Figure 3.20 The cholinesterase inhibitory activities of xanthyletin (**6**) at the final concentrations of 0.5, 0.1, and 0.05 mg/mL. Data are express as means ($n = 2$)

Figure 3.21 The cholinesterase inhibitory activities of crenulatin (**7**) at the final concentrations of 0.5, 0.1, and 0.05 mg/mL. Data are express as means ($n = 2$)

Figure 3.22 The cholinesterase inhibitory activities of 5-hydroxynoracronycine (**8**) at the final concentrations of 0.5, 0.1, and 0.05 mg/mL. Data are express as means ($n = 2$)

Figure 3.23 The cholinesterase inhibitory activities of citracridone-I (**9**) at the final concentrations of 0.5, 0.1, and 0.05 mg/mL. Data are express as means ($n = 2$)

Figure 3.24 The cholinesterase inhibitory activities of umbelliferone (**10**) at the final concentrations of 0.5, 0.1, and 0.05 mg/mL. Data are express as means ($n = 2$)
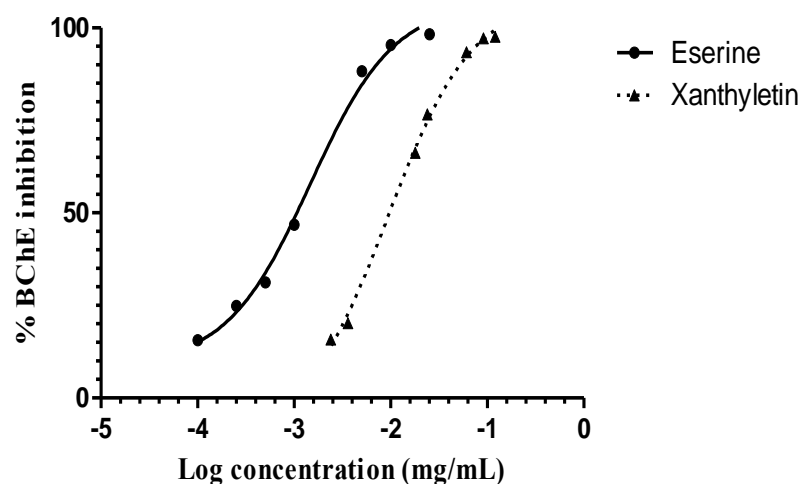
Figure 3.25 Dose response curves of eserine (the standard inhibitor) and xanthyletin (**6**) against butyrylcholinesterase. Data are expressed as means ($n = 2$)

To determine the mode of BChE inhibition of xanthyletin (**6**), this substance was further evaluated for its kinetic studies. The Lineweaver-Burk plot of xanthyletin (Figure 3.26) demonstrated the decreased v_{max} values from the reciprocal of the Y-intercept, and the increased K_m values from the negative reciprocal of X-intercept. These results identified the mixed inhibition which the inhibitor may bind to the same active site of substrate or allosteric site of enzyme, and also binds to the enzyme whether or not the enzyme has already bound to the substrate. Moreover, this study was the first report of xanthyletin as the mixed inhibitor towards BChE.
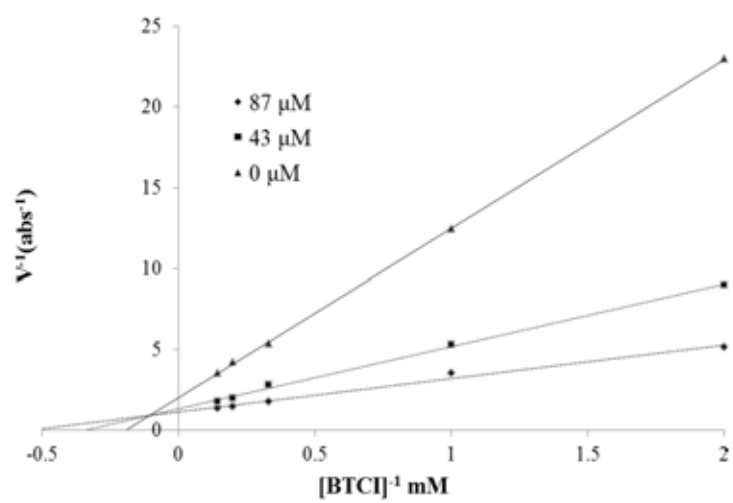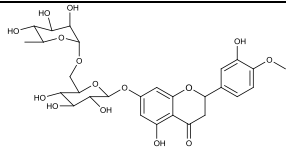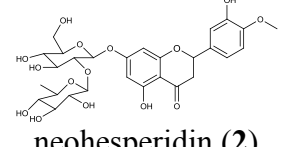
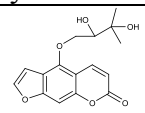**Figure 3.26** The Lineweaver-Burk plot of xanthyletin (**6**)

CHAPTER IV
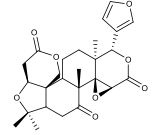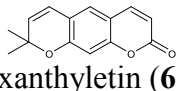
CONCLUSION

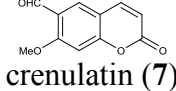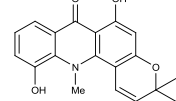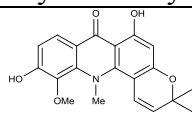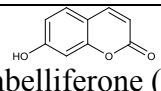In this study, the leaves and roots of *C. hystrix* were determined the chemical components, and evaluated for their anti-cholinesterase activities. Ten isolated substances were obtained from the BuOH and dichloromethane extracts of leaves, and EtOAc extract of the roots. Compounds **1-2** and **3-4** were obtained from the BuOH and dichloromethane extracts from the leaves, respectively. The EtOAc extract from the roots gave compounds **5-10**. The structures of these isolated compounds were fully elucidated on the spectral data (^{1}H NMR and ^{13}C NMR), and by comparison with published data. These isolated compounds were hesperidin (**1**), neohesperindin (**2**), alkyl alcohol (**3**), oxypeucedanin hydrate (**4**), limonin (**5**), xanthyletin (**6**), crenulatin (**7**), 5-hydroxynoracronycine (**8**), citracridone-I (**9**), and umbelliferone (**10**). All chemical structures of isolated compounds are displayed in Table 4.1.

All isolated compounds were further evaluated for their acetylcholinesterase (AChE) and butyrycholinesterase (BChE) inhibitory activities. Xanthyletin (**6**) showed the highest inhibition towards BChE with the IC_{50} value of 37.4 μM which was 14-folds higher than that of eserine (IC_{50} = 2.7 μM), and conducted as a mixed inhibitory mode. On the contrary, the other compounds showed low-to-moderate activities (% inhibition < 50%), and low solubility under assay condition. In this study, the BChE inhibitory activity and the inhibitory mode of xanthyletin as mixed inhibitor were reported for the first time. Although, isolated compounds from *C. hystrix* showed medium anti-cholinesterase activities comparing to eserine, but they were purified from natural plant which is safe for health. Moreover, previous reports indicated that neohesperidin (**2**) showed the anti-oxidant, anti-viral, anti-allergic, anti-tyrosinase, and anti-bacterial activities (Suarez *et al.*, 1998; Kim *et al.*, 2000; Itoh *et al.*, 2009; Itoh *et al.*, 2009; Alapont *et al.*, 2000). Oxypeucedanin hydrate (**4**) possessed anti-fungal, anti-proliferative, anti-microbial, anti-oxidant, and GABA-transaminase inhibitory activities (Marston and Hostettmann 1995; Kim *et al.*, 2007; Dongfack *et al.*, 2012; Piao *et al.*, 2004; Choi *et al.*, 2005). Xanthyletin also showed

the anti-inflammatory, anti-fungus, anti-bacterial, cytotoxic activities (Chan *et al.*, 2010; Khan *et al.*, 1985; Godoy *et al.*, 2005; Chiang *et al.*, 2010; Magiatis *et al.*, 1998). These results suggested that *C. hystrix* and xanthyletin should be further evaluated for their *in vivo* activity, and developed to be an effective option for the treatment of AD and other diseases, or use as supplement dietary.

Table 4.1 Isolated substances (**1-11**) from *C. hystrix* leaves and roots

Substance	% Inhibition at 0.5 mg/mL		IC$_{50}$ value (μM)	
	AChE	**BChE**	**AChE**	**BChE**
hesperidin (**1**)	59.21	28.43	nt	nt
neohesperidin (**2**)	70.00	13.51	160.1	nt
alkyl alcohol (**3**)	26.74	16.39	nt	nt
oxypeucedanin hydrate (**4**)	58.47	62.47	570.3	260.8
limonin (**5**)	20.57	18.11	nt	nt
xanthyletin (**6**)	77.89	92.45	116.2	37.4
crenulatin (**7**)	35.69	36.99	nt	nt
5-hydroxynoracronycine (**8**)	29.48	53.92	nt	nt
citracridone-I (**9**)	42.63	83.91	nt	nt
umbelliferone (**10**)	30.38	42.32	nt	nt

nt = not test

REFERENCES

Alapont, C.G., Domenech, R.G., Gálvez, J., Ros, M.J., Wolski, S., and Gracía, M.D. Molecular topology: a useful tool for the search of new antibacterials. Bioorganic and Medicinal Chemistry Letters 10 (2000): 2033-2036.

Alzheimer's Disease International. World Alzheimer's report 2010: the global economic impact of dementia. London: Alzheimer's Disease International, 2010.

Atack, J.R., Perry, E.K., Bonham, J.R., Candy, J.M., and Perry, R.H. Molecular forms of acetylcholinesterase in the aged human central nervous system. Journal of Neurochemistry 47 (1986): 263-277.

Basa, S.C., and Tripathy, R.N. Constituents of *Hesperathusa crenulata*. Journal of Natural Products 45 (1982): 503-504.

Bascetta, E., and Gunstone, F.D. ^{13}C chemical shifts of long-chain epoxides, alcohols and hydroperoxides. Chemistry and Physics of Lipids 36 (1985): 253-261.

Brunel, J.M. Scope, limitations and mechanistic aspects in the selective homogenous palladium-catalyzed reduction of alkanes under transfer hydrogen condition. Tetrahedron 63 (2007): 3899-3906.

Cazal, C.M. et al. Isolation of xanthyletin, an inhibitor of ants' symbiotic fungus, by high-speed counter-current chromatography. Journal of Chromatography A 1216 (2009): 4307-4312.

Chan, Y.Y., Li, C.H., Shen, Y.C., and Wu, T.S. Anti-inflammatory principles from the stem and root barks of *Citrus medica*. Chemical and Pharmaceutical Bulletin 58 (2010): 61065.

Ching, L.S., and Mohamed, S. Alpha-tocopherol content in 62 edible tropical plants. Journal of Agricultural and Food Chemistry 49 (2001): 3101-3105.

Chaiyana, W., Saeio, K., Hennink, W.E., and Okonogi, S. Characterization of potent anticholinesterase plant oil based microemulsion. International Journal of Pharmaceutics 401 (2010): 32-40.

Chaiyana, W., and Okonogi, S. Inhibition of cholinesterase by essential oil from food plant. Phytomedicine 19 (2012): 836-839.

Chiang, C.C., Cheng, M.J., Peng, C.F., Huang, H.Y., and Chen, I.S. A novel dimeric coumarin analog and antimycobacterial constituents from *Fatoua pilosa*. Chemistry and Biodiversity 7 (2010): 1728-1736.

Choi, S.Y. et al. *In vitro* GABA-transaminase inhibitory compounds from the root of *Angelica dahurica*. Phytotherapy Research 19 (2005): 839-845.

Clayton, T., Saralamp, P., Chuakul, W., and Temsiririkkul, R. Medicinal plants in Siri Ruckhachati Garden Thailand. Bangkok: Faculty of Pharmacy, Mahidol University, 1994.

Cummings, J.L. Alzheimer's disease. The New England Journal of Medicine 351 (2004): 56-67.

Darvesh, S., Hopkins, D., and Geula, C. Neurobiology of butyrylcholinesterase. Neuroscience 4 (2003): 131-138.

Dongfack, M.D.J. et al. A new sphingolipid and furanocoumarins with antimicrobial activity from *Ficus exasperata*. Chemical and Pharmaceutical Bulletin 60 (2012):1072-1075.

Elliott, S., and Brimacombe, J. The medicinal plants of Gunung Leuser National Park. Journal of Ethnopharmacology 19 (1987): 285-317.

Ellman, G.L., Courtney, K.D., Andres, Jr.V., and Featherstone, R. A new and rapid colorimetric determination of acetylcholinesterase activity. Biochemical Pharmacology 7 (1961): 88-95.

Fortin, H. et al. In vitro antiviral activity of thirty-six plants from La Réunion Island. Fitoterapia 73 (2002): 346-350.

Frank, B., and Gupta, S. A review of antioxidant and Alzheimer's disease. Annals of Clinical Psychiatry 17 (2005): 269-286.

Furukawa, H., Yogo, M., and Wu, T.S. Acridone alkaloids X. ^{13}C-Nuclear magnetic resonance spectra of acridone alkaloids. Chemical and Pharmaceutical Bulletin 31 (1983): 3084-3090.

Gertz, H.J., and Kiefer, M. Review about *Ginkgo biloba* special extract EGb 761 (Ginkgo). Current Pharmaceutical Design 10 (2004): 261-264.

Godoy, M.F.P. et al. Inhibition of the symbiotic fungus of leaf-cutting ants by coumarins. Journal of the Brazilian Chemical Society 16 (2005): 669-672.

Hamdan, D. et al. Chemical composition and biological activity of *Citrus jambhiri* Lush. Food Chemistry 127 (2011): 394-403.

Harkar, S., Razdan, T.K., and Waight, E.S. Steroids, chromone and coumarins from *Angelica officinalis*. Phytochemistry 23 (1984): 419-426.

Heinrich, M., and Teoh, H.L. Galanthamine from snowdrop – the development of a modern drug against Alzheimer's disease from local Caucasian knowledge. Journal of Ethnopharmacology 92 (2004): 147-162.

Ingkaninan, K., Temkitthawon, P., Chuenchom, K., Yuyaem, T., and Thongnoi, W. Screening for acetylcholinesterase inhibitory activity in plants used in Thai traditional rejuvenating and neurotonic remedies. Journal of Ethnopharmacology 89 (2003): 261-264.

Itoh, K. et al. Inhibitory effects of *Citrus hassaku* extract and its flavanone glycosides on melanogenesis. Biological and Pharmaceutical Bulletin 32 (2009): 410-415.

Itoh, K., Masuda, M., Naruto, S., Murata, K., and Matsuda, H. Antiallergic activity of unripe *Citrus hassaku* fruits extract and its flavanone glycosides on chemical substance-induced dermatitis in mice. Journal of Natural Medicines 63 (2009): 443-450.

Lahiri, D.K., farlow, M.R., Greig, N.H., and Sambamurti, K. Current drug targets for Alzheimer's disease treatment. Drug Development Research 56 (2002): 267-281.

Kang, S.Y., Lee, K.Y., Sung, S.H., Park, S.M., and Kim, Y.C. Coumarins isolated from *Angelica gigas* inhibit acetylcholinesterase: structure-activity relationships. Journal of Natural Products 64 (2001): 683-685.

Khan, A.J., Kunesch, G., Chuilon, S., and Ravise, A. Structure and biological activity of xanthyletin a new phytoalexin of citrus. Fruits 40 (1985): 807-811.

Khan, M.T.H. et al. Cholinesterase inhibitory activities of some flavonoid derivatives and chosen xanthone and their molecular docking studies. Chemico-Biological Interactions 181 (2009): 383-389.

Kim, D.H., Song, M.J., Bae, E.H., and Han, M.J. Inhibitory effect of herbal medicines on rotavirus infectivity. Biological and Pharmaceutical Bulletin 23 (2000): 356-358.

Kim, Y.K., Kim, Y.S., and Ryu, S.Y. Antiproliferative effect of furanocoumarins from the root of *Angelica dahurica* on cultured human tumor cell lines. Phytotherapy Research 21 (2007): 288-290.

Kong, L.Y., Li, Y., Min, Z.D., Li, X., and Zhu, T.R. Coumarins from *Peucedanum praeruptorum*. Phytochemistry 41 (1996): 1422-1426.

Lim S.S., Han, S.M., Kim, S.Y., Bae, Y.S., and Kang, I.J. Isolation of acetylcholinesterase inhibitors from the flowers of *Chrysanthemum indicum* Linne. Food Science and Biotechnology 16 (2007): 265-269.

Magiatis, P. et al. Synthesis and cytotoxic activity of pyranocoumarins of the seselin and xanthyletin series. Journal of Natural Products 61 (1998): 982-986.

Maltese, F., Erkelens, C., Kooy, F., Choi, Y.H., and Verpoorte, R. identification of natural epimeric flavanone glycosides by NMR spectroscopy. Food Chemistry 116 (2009): 575-579.

Manosroi, J., Dhumtanom, P., and Manosroi, A. Anti-proliferative activity of essential oil extracted from Thai medicinal plants on KB and P388 cell lines. Cancer Letters 235 (2006): 114-120.

Marston, A., and Hostettmann, K. Isolation of antifungal and larvicidal constituents of *Diplolophium buchanani* by centrifugal partition chromatography. Journal of Natural Products 58 (1995): 128-130.

Miean, K.H., and Mohamed, S. Flavonoid (myricetin, quercetin, kaempferol, luteolin, and apigenin) content of edible tropical plants. Journal of Agricultural and Food Chemistry 49 (2001): 3106-3112.

Min, Y.D., Kwon, H.C., Yang, M.C., Lee, K.H., Choi, S.U., and Lee K.R. Isolation of limonoids and alkaloids from *Phellodendron amurense* and their multidrug resistance (MDR) reversal activity. Archives of Pharmacal Research 30 (2007): 58-63.

Murakami, A., Jiwajinda, S., Koshimizu, K., and Ohigashi, H. Screening for in vitro anti-tumor promoting activities of edible plants from Thailand. Cancer Letters 95 (1995a): 139-146.

Murakami, A., Nakamura, Y., Koshimizu, K., and Oshigashi, H. Glyceroglycolipids from *Citrus hystrix*, a traditional herb in Thailand, potently inhibit the tumor-promoting activity of 12-*O*-tetradecanoylphorbol 13-acetate in mouse skin. Journal of Agricultural and Food Chemistry 43 (1995b): 2779-2783.

Murakami, A. et al. Identification of coumarins from the fruit of *Citrus hystrix* DC as inhibitors of nitric oxide generation in mouse macrophage RAW 264.7 cells. Journal of Agricultural and Food Chemistry 47 (1999): 333-339.

Oda, Y. Choline acetyltranferase: the structure, distribution and pathologic changes in the central nervous system. Pathology International 49 (1999): 921-937.

Ogawa, K. et al. Evaluation of auraptene content in citrus fruits and their products. Journal of Agricultural and Food Chemistry 48 (2000): 1763-1769.

Ong, C.Y. et al. Systematic analysis of in vitro photo-cytotoxic activity in extracts from terrestrial plants in Peninsula Malaysia for photodynamic therapy. Journal of Photochemistry and Photobiology B: Biology 96 (2009): 216-222.

Panthong, K., Srisud, Y., Rukachaisirikul, V., Hutadilok-Towatana, N., Voravuthikunchai, S.P., and Tewtrakul, S. Benzene, coumarin and quinolinone derivatives from roots of *Citrus hystrix*. Phytochemistry 88 (2013): 79-84.

Perry, E.K., Perry, R.H., Blessed, G., and Tomlinson, B.E. Changes in brain cholinesterase in senile dementia of Alzheimer type. Neuropathology and Applied Neurobiology 4 (1978): 273-277.

Piao, X.L., Park, I.H., Baek, S.H., Kim, H.Y., Park, M.K., and Park, J.H. antioxidative activity of furanocoumarins isolated from *Angelicae dahuricae*. Journal of Ethnopharmacology 93 (2004): 243-246.

Piyachatuwat, P., Glinsukon, T., and Chanjarunee, A. Antifertility effect of *Citrus hystrix* DC. Journal of Ethnopharmacology 13 (1985): 105-110.

Rhee, I.K., Meent, M., Ingkaninan, K., and Verpoorte, R. Screening for acetylcholinesterase inhibitors from Amaryllidaceae using silica gel thin-layer chromatography in combination with bioactivity staining. Journal of Chromatography A 915 (2001): 217-223.

Salah, S.M., and Jäger, A.K. Screening of traditionally used Lebanese herbs for neurological activities. Journal of Ethnopharmacology 97 (2005): 145-149.

Suarez, J., Herrera, M.D., and Marhuenda, E. *In vitro* scavenger and antioxidant properties of hesperidin and neohesperidin dihydrochalcone. Phytomedicine 5 (1998): 469-473.

Tildesley, N.T.J. et al. *Salvia lavandulaefolia* (Spanish sage) enhance memory in healthy young volunteers. Pharmacology Biochemistry and Behavior 75 (2003): 669-674.

Wannisorn, B., Jarikasem, S., Siriwangchai, T., and Thubthimthed, S. Antibacterial properties of essential oils from Thai medicinal plants. Fitoterapia 76 (2005): 233-236.

Wszelaki, N., Paradowska, K., Jamróz, M., Granica, S., and Kiss, A.K. Bioactivity-guided fractionation for the butyrylcholinesterase inhibitory activity of furanocoumarins fron *Angelica archangelica* L. roots and fruits. Journal of Agricultural and Food Chemistry 59 (2011): 9186-9193.

Wong, S.P., Leong, L.P., and Koh, J.H.W. Antioxidant activities of aqueous extracts of selected plants. Food Chemistry 99 (2006): 775-783.

Wu, T.S., Kuoh, C.S. and Furukawa, H. Acridone alkaloids VI. The constitutents of *Citrus depressa*. Isolation and structure elucidation of new acridone alkaloids from *Citrus* genus. Chemical and Pharmaceutical Bulletin 31 (1983): 896-900.

Wu, T.S., and Furukawa, H. Acridone alkaloids VII. Constitutents of *Citrus sinensis* Osbeck var. *brasiliensis* Tanaka. Isolation and characterization of three new acridone alkaloids, and a new coumarin. Chemical and Phamaceutical Bulletin 31 (1983): 901-906.

Youkwan, J., Sutthivaiyakit, S., and Sutthivaiyakit, P. Citrusosides A-D and furanocoumarins with cholinesterase inhibitory activity from the fruit peels of *Citrus hystrix*. Journal of Natural Products 73 (2010): 1879-1883.

APPENDIX
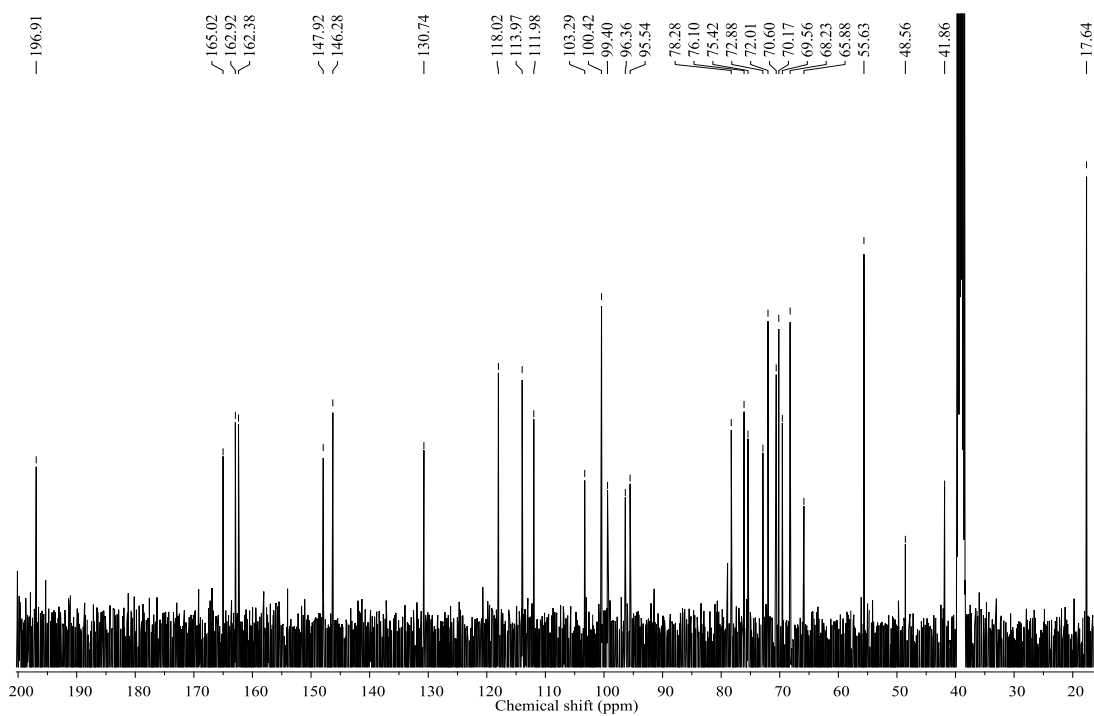
Figure A-1 The ^{13}C-NMR spectrum (DMSO-d_6) of hesperidin (**1**)
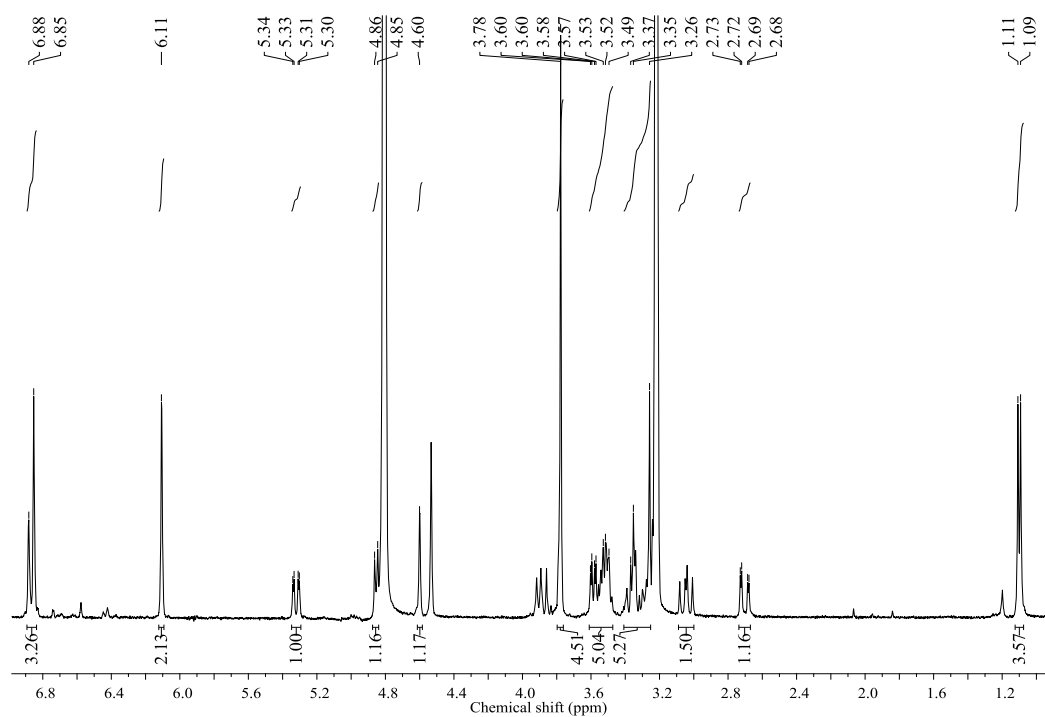
Figure A-2 The ^{1}H-NMR spectrum (CD$_3$OD) of hesperidin (**1**)
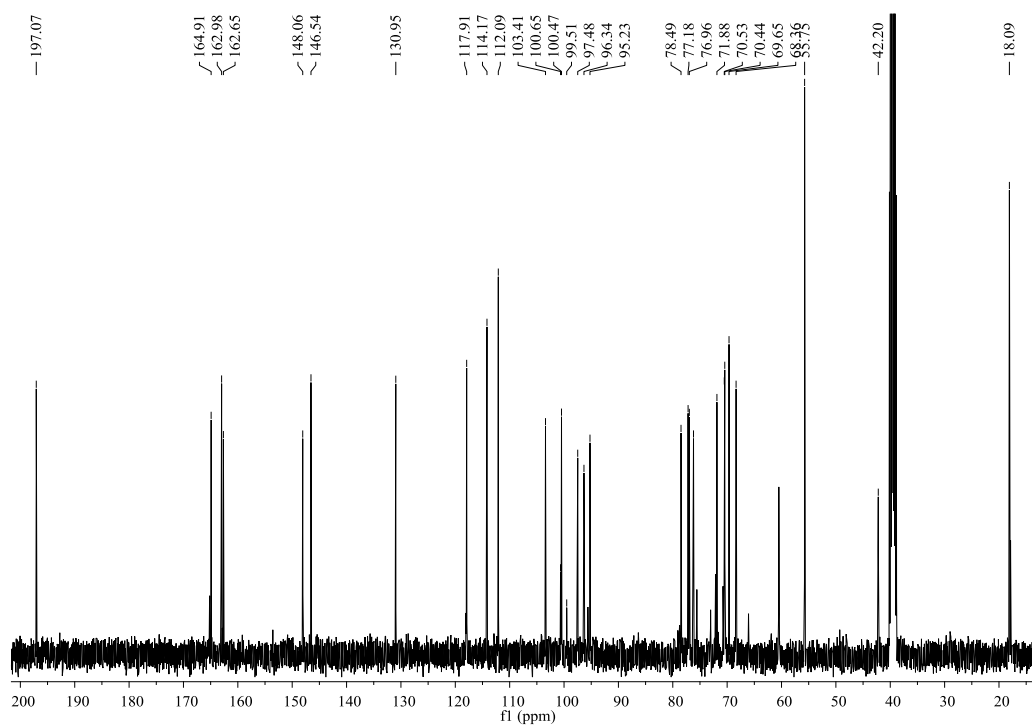
Figure A-3 The ^{13}C-NMR spectrum (DMSO-d_6) of neohesperidin (**2**)
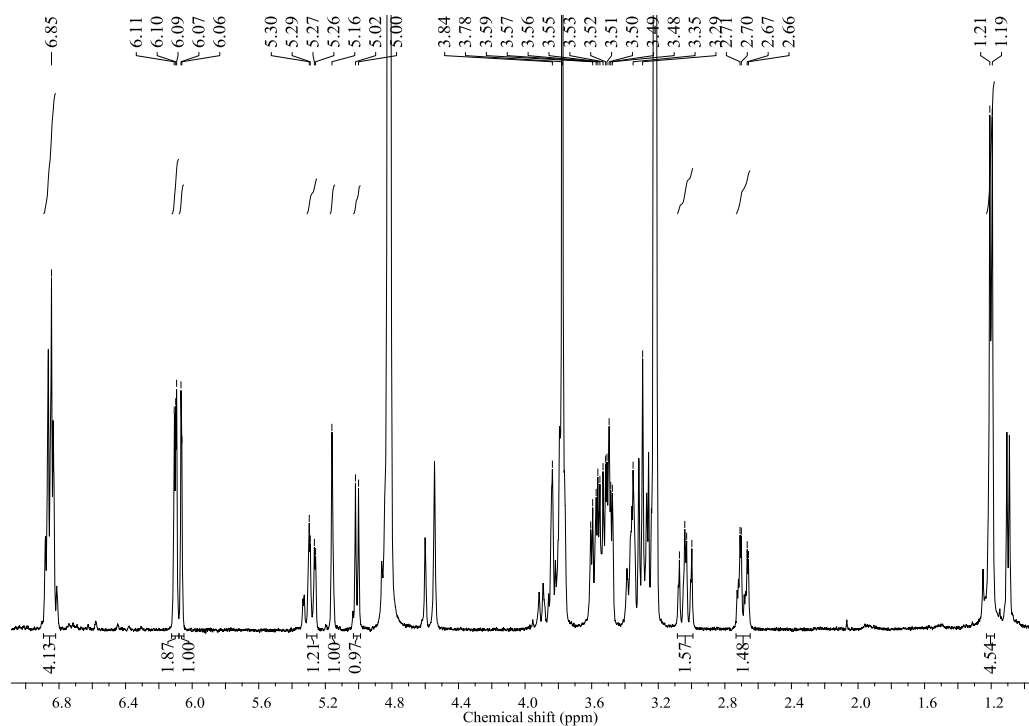
Figure A-4 The ^{1}H-NMR spectrum (CD$_3$OD) of neohesperidin (**2**)
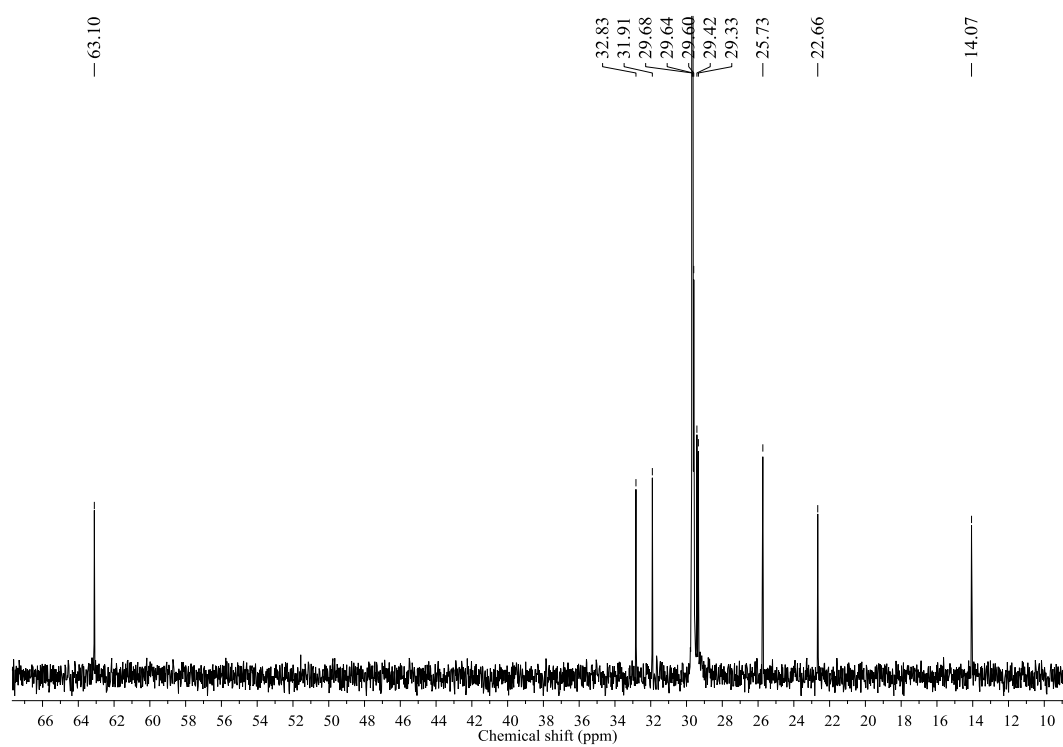
Figure A-5 The ^{13}C-NMR spectrum (CDCl$_3$) of alkyl alcohol (**3**)
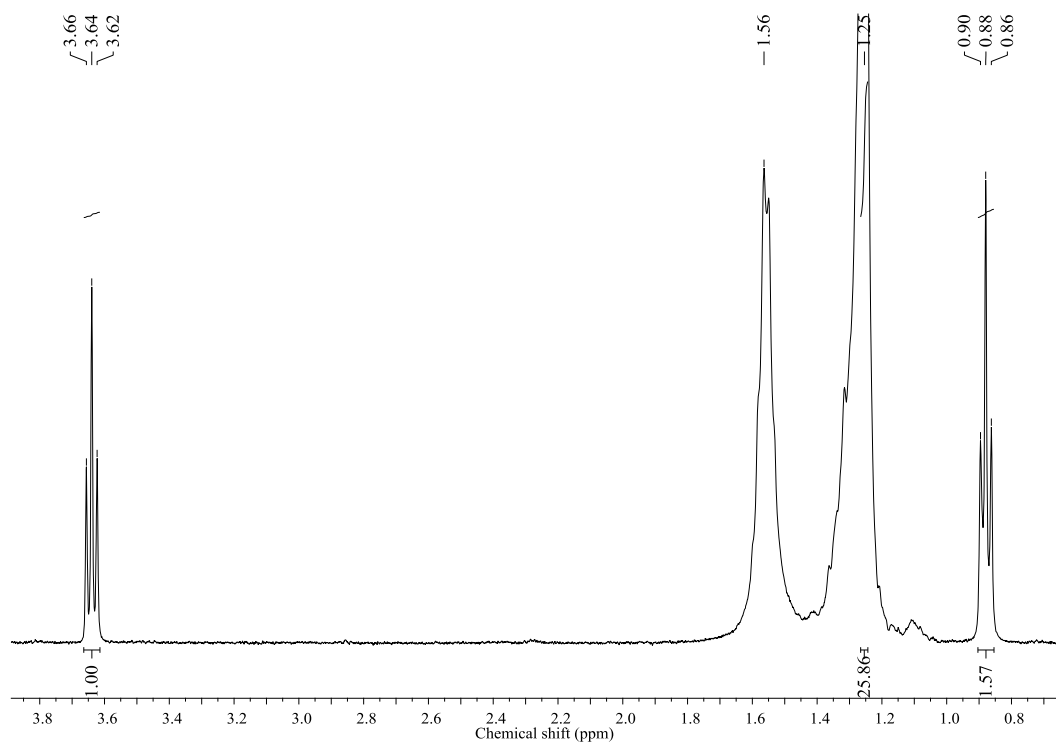
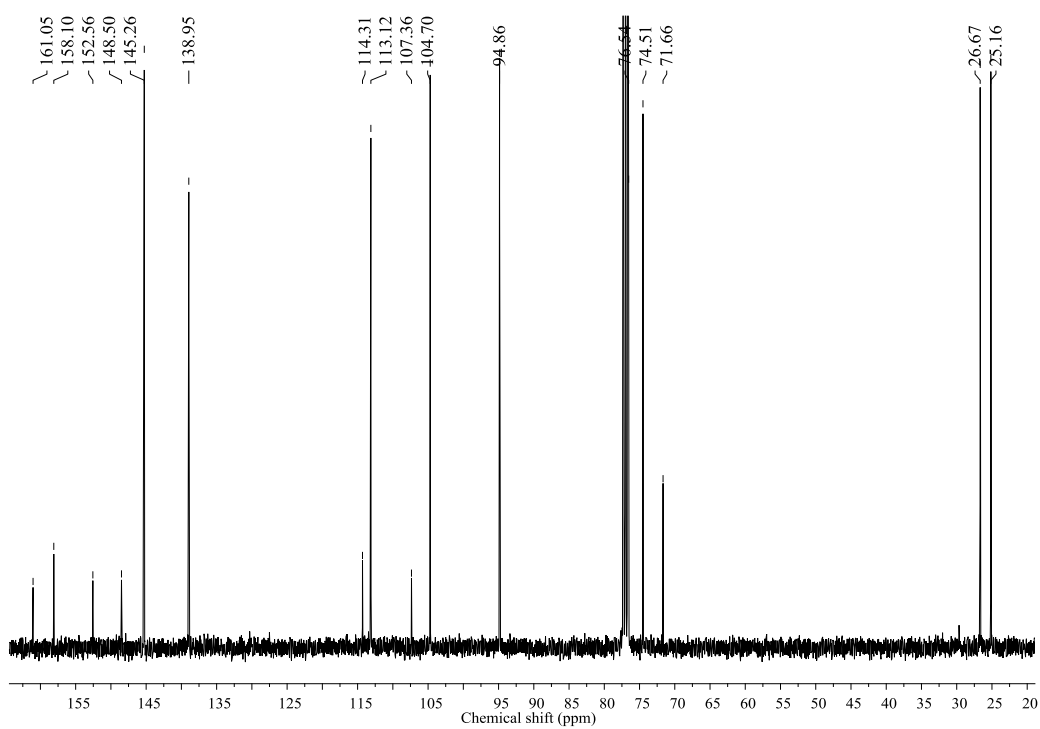**Figure A-6** The ^{1}H-NMR spectrum (CDCl$_3$) of alkyl alcohol (**3**)

Figure A-7 The ^{13}C-NMR spectrum (CDCl$_3$) of oxypeucedanin hydrate (**4**)
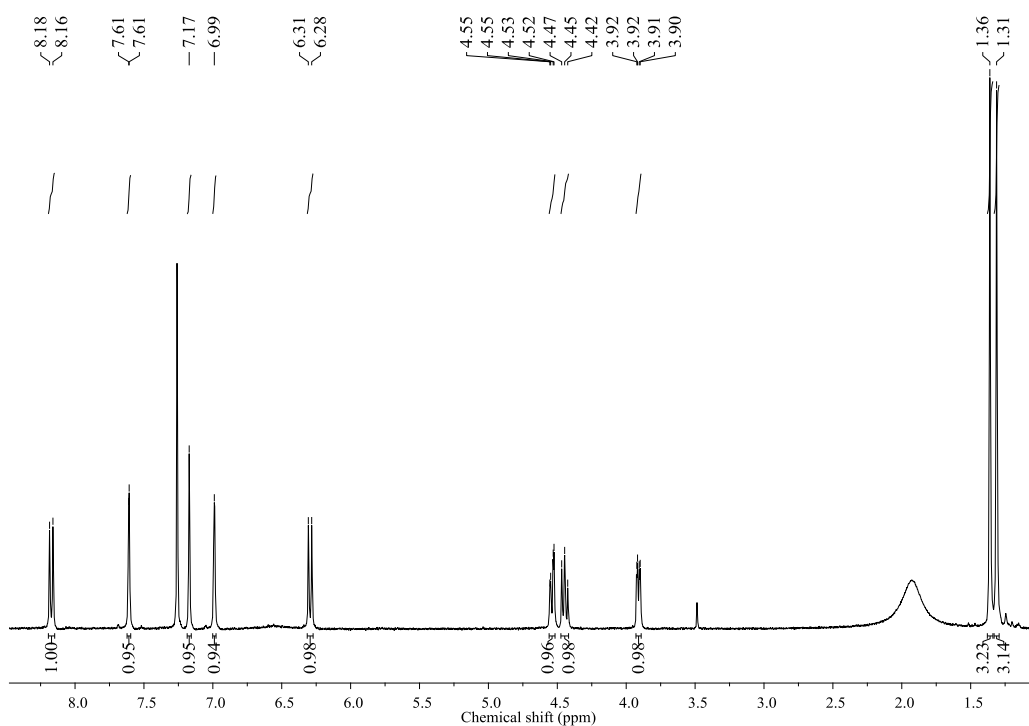
Figure A-8 The ^{1}H-NMR spectrum (CDCl$_3$) of oxypeucedanin hydrate (**4**)
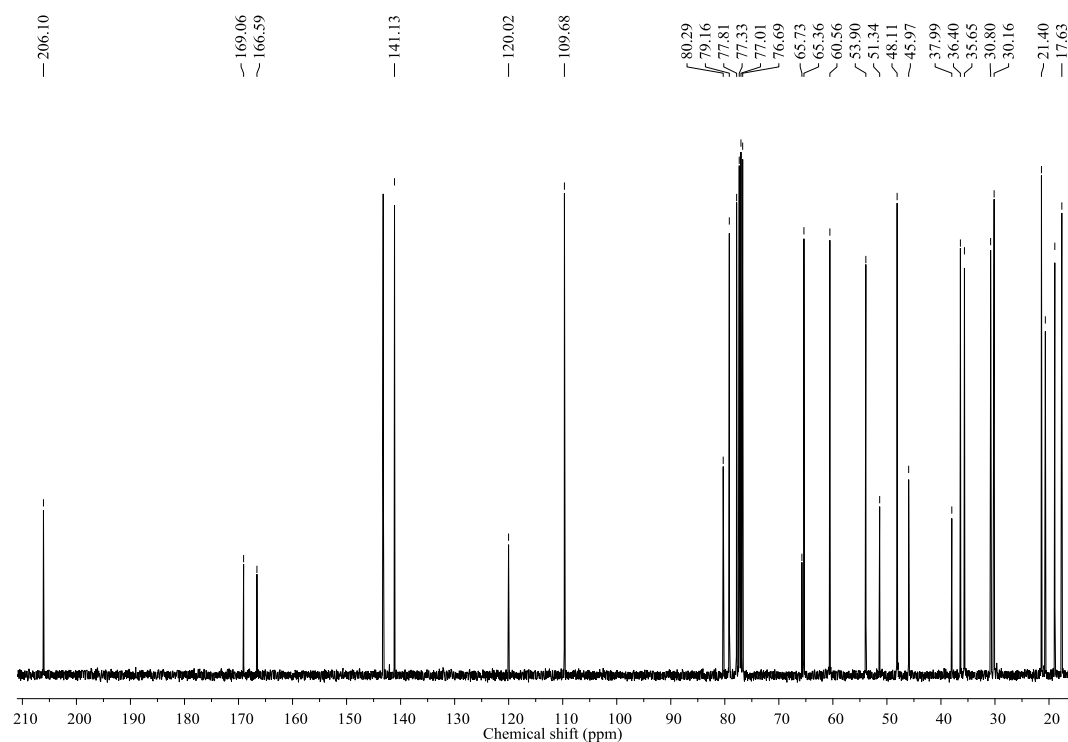
Figure A-9 The ^{13}C-NMR spectrum (CDCl$_3$) of limonin (**5**)
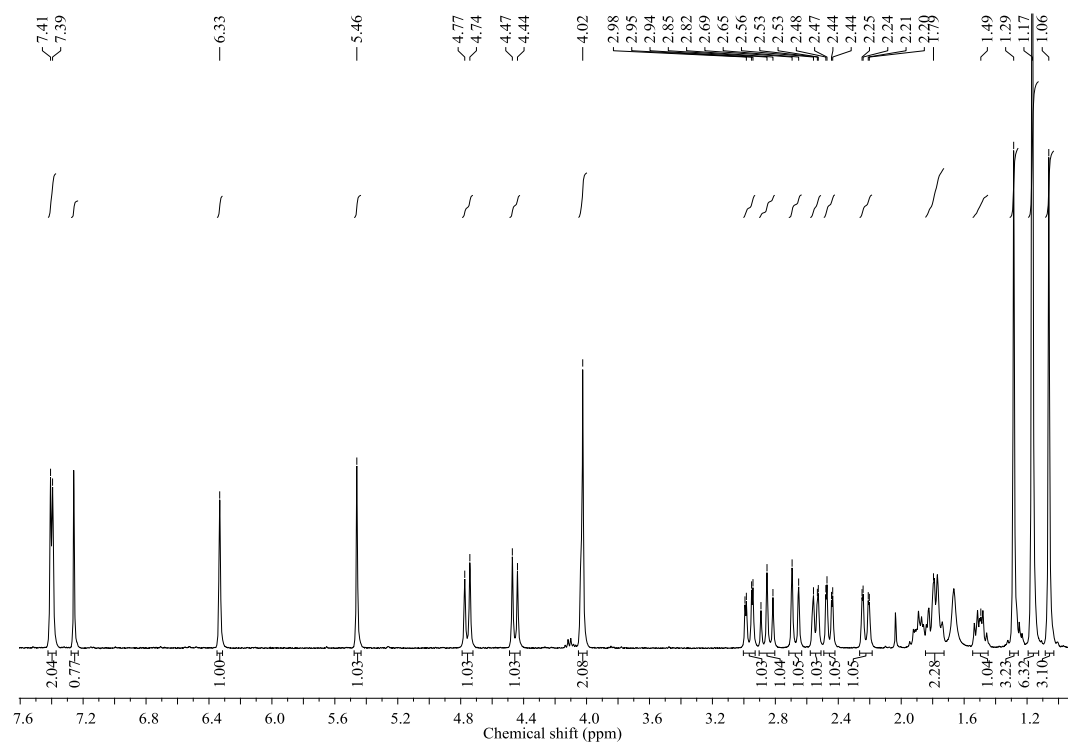
Figure A-10 The ^{1}H-NMR spectrum (CDCl$_3$) of limonin (**5**)
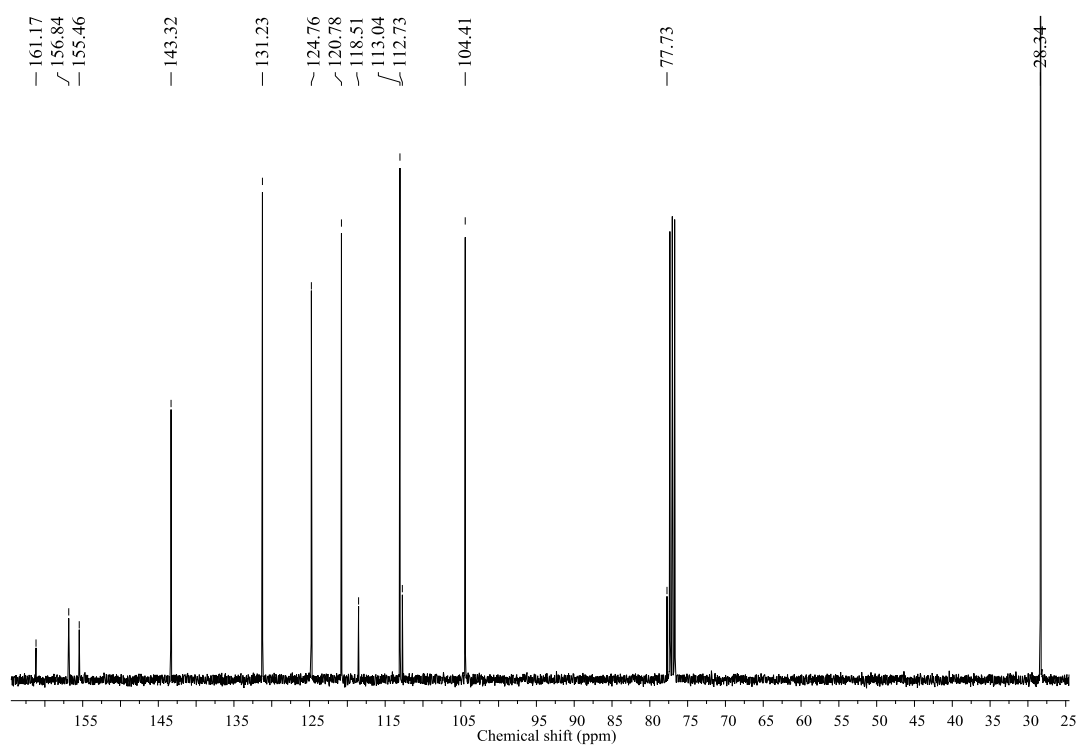
Figure A-11 The ^{13}C-NMR spectrum (CDCl$_3$) of xanthyletin (**6**)
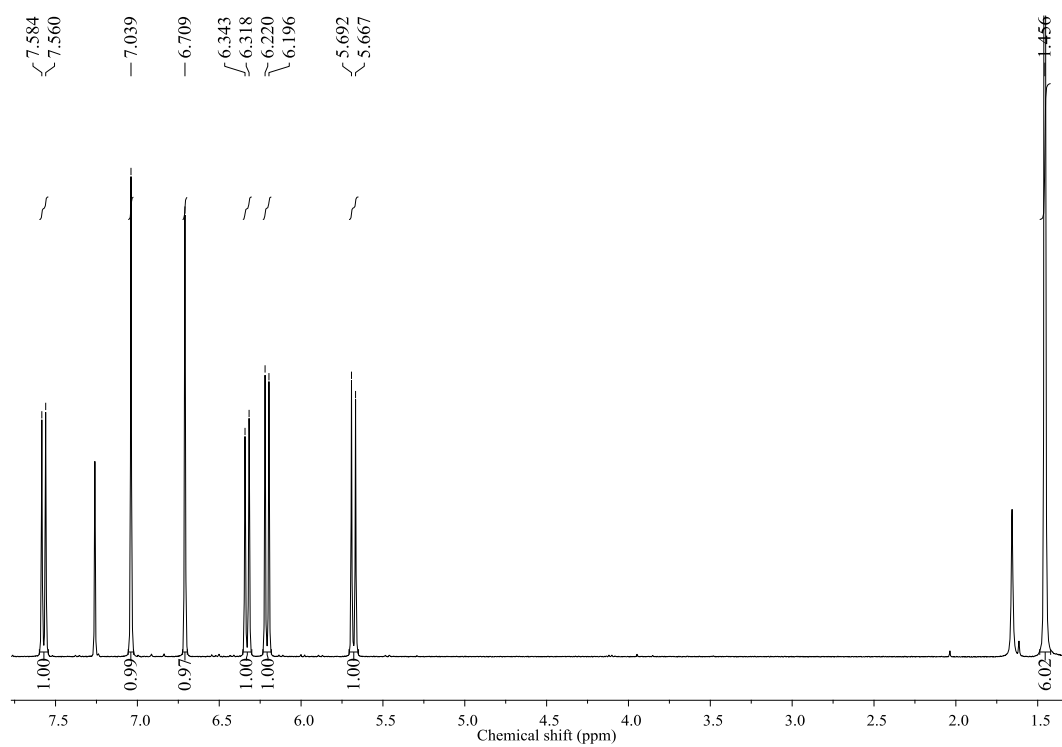
Figure A-12 The ^{1}H-NMR spectrum (CDCl$_3$) of xanthyletin (**6**)
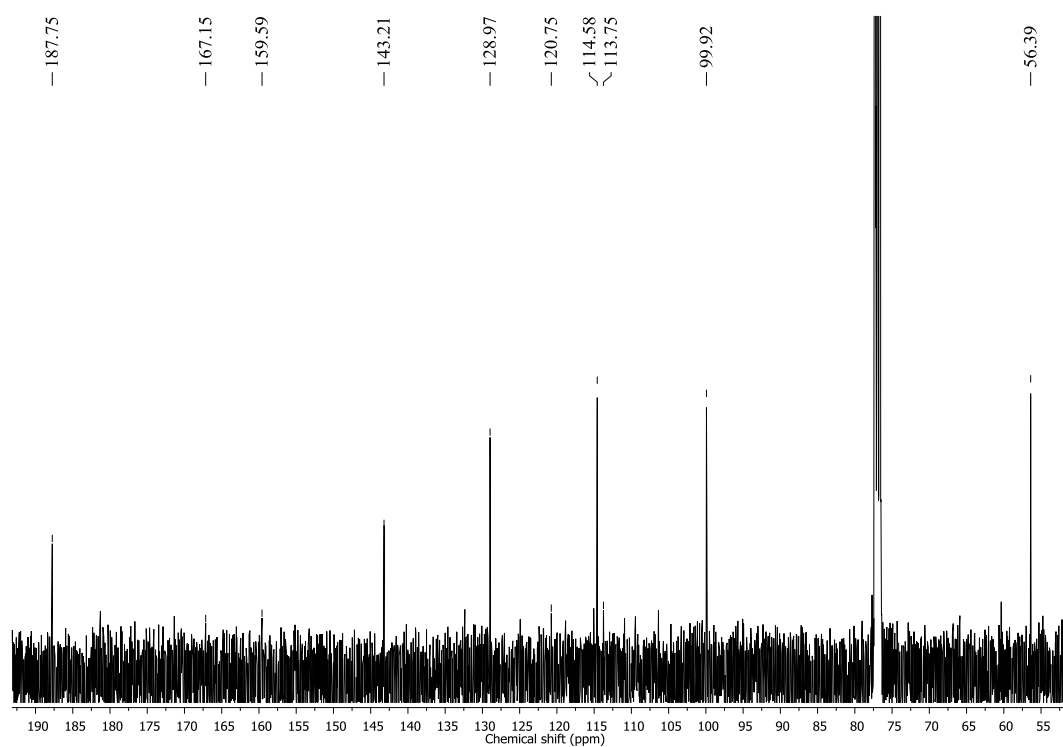
Figure A-13 The ^{13}C-NMR spectrum (CDCl$_3$) of crenulatin (**7**)
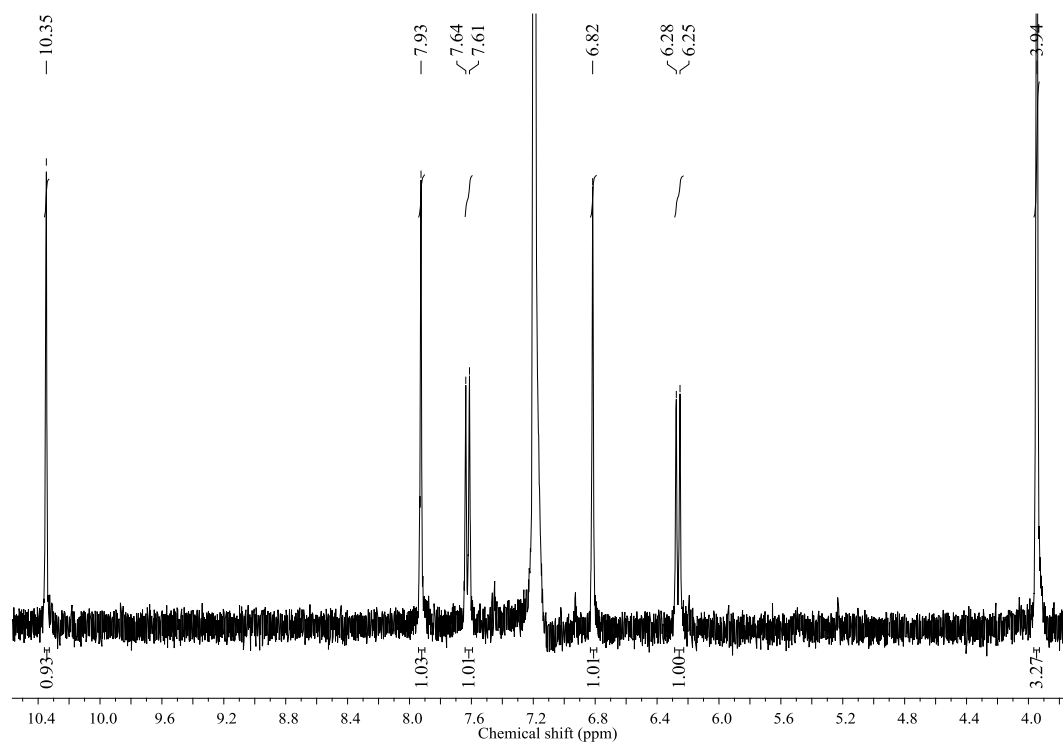
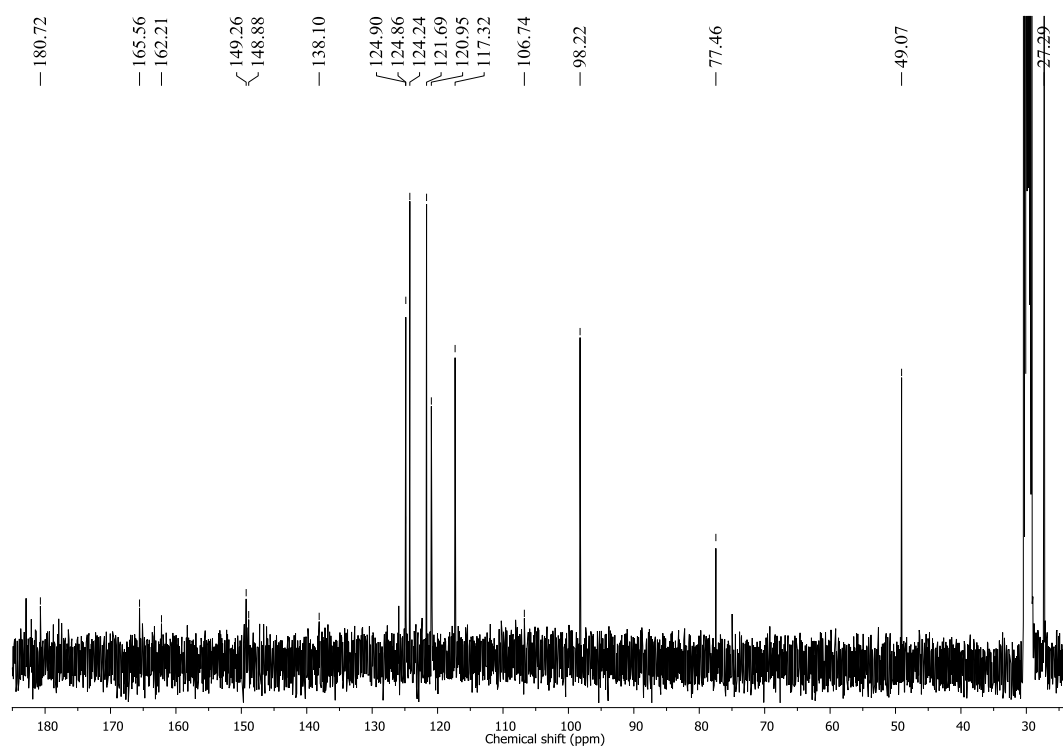**Figure A-14** The ^{1}H-NMR spectrum (CDCl$_3$) of crenulatin (**7**)

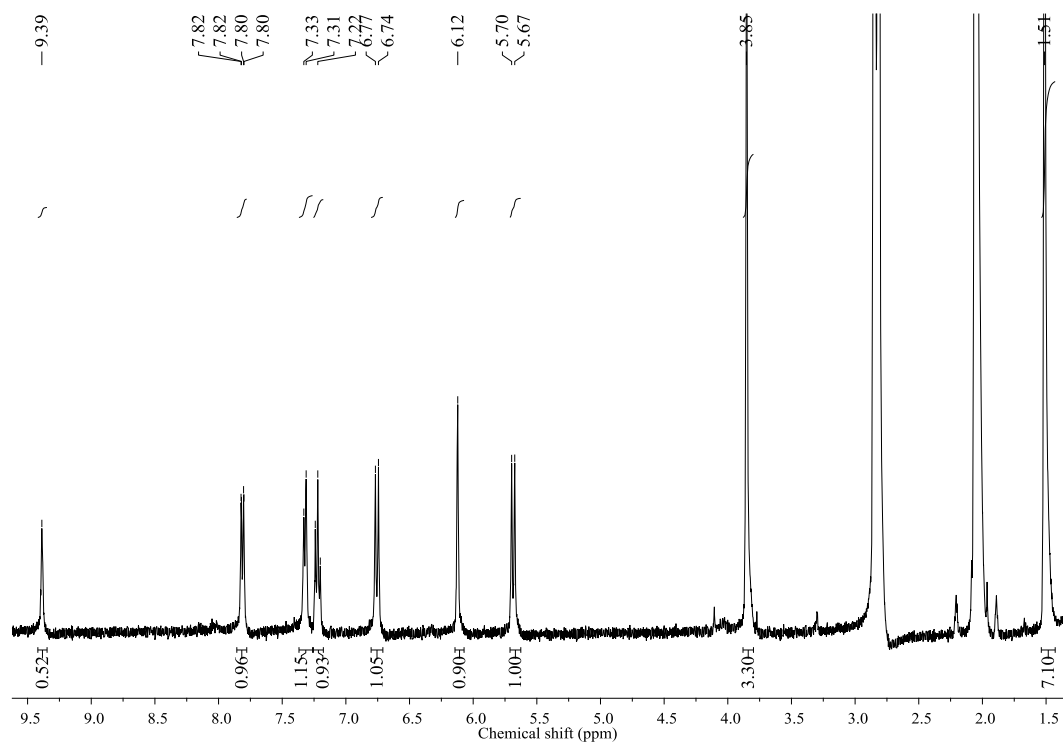**Figure A-15** The ^{13}C-NMR spectrum (acetone-d_6) of 5-hydroxynoracronycine (**8**)

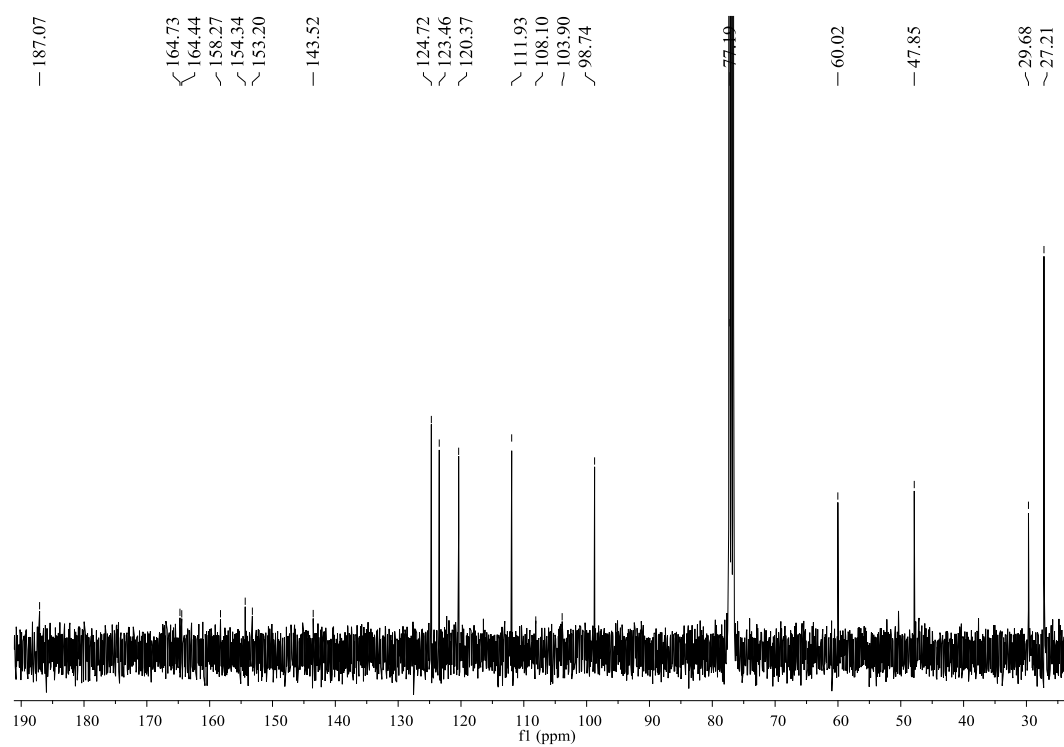**Figure A-16** The ^{1}H-NMR spectrum (acetone-d_6) of 5-hydroxynoracronycine (**8**)

Figure A-17 The ^{13}C-NMR spectrum (CDCl$_3$) of citracridone-I (**9**)
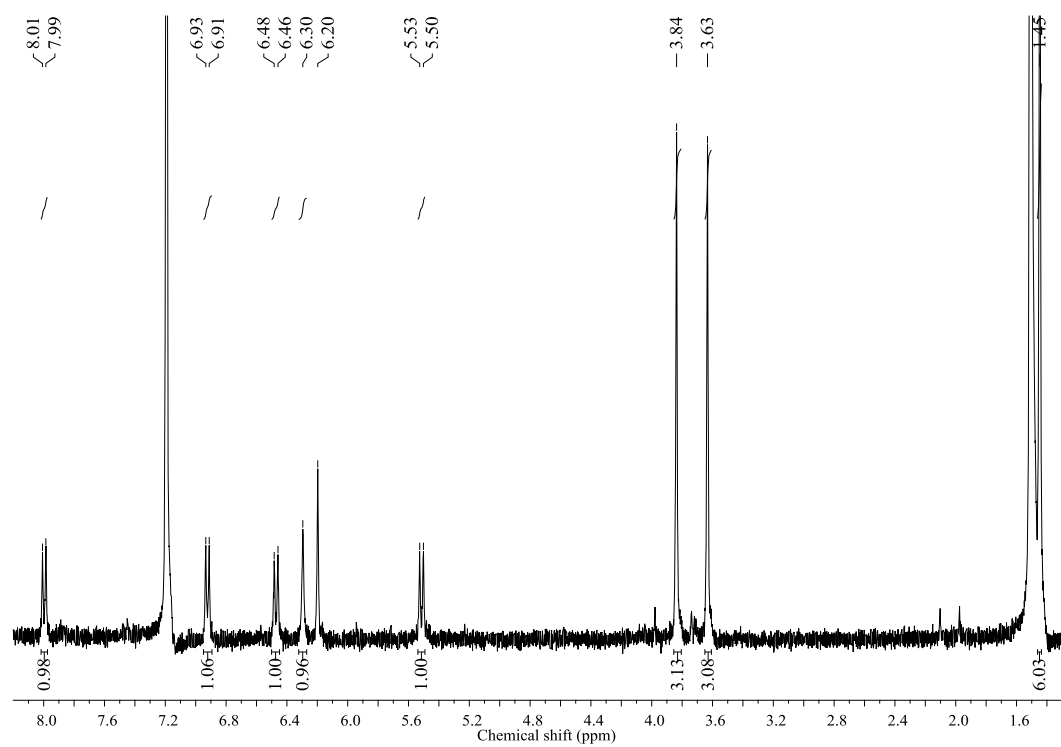

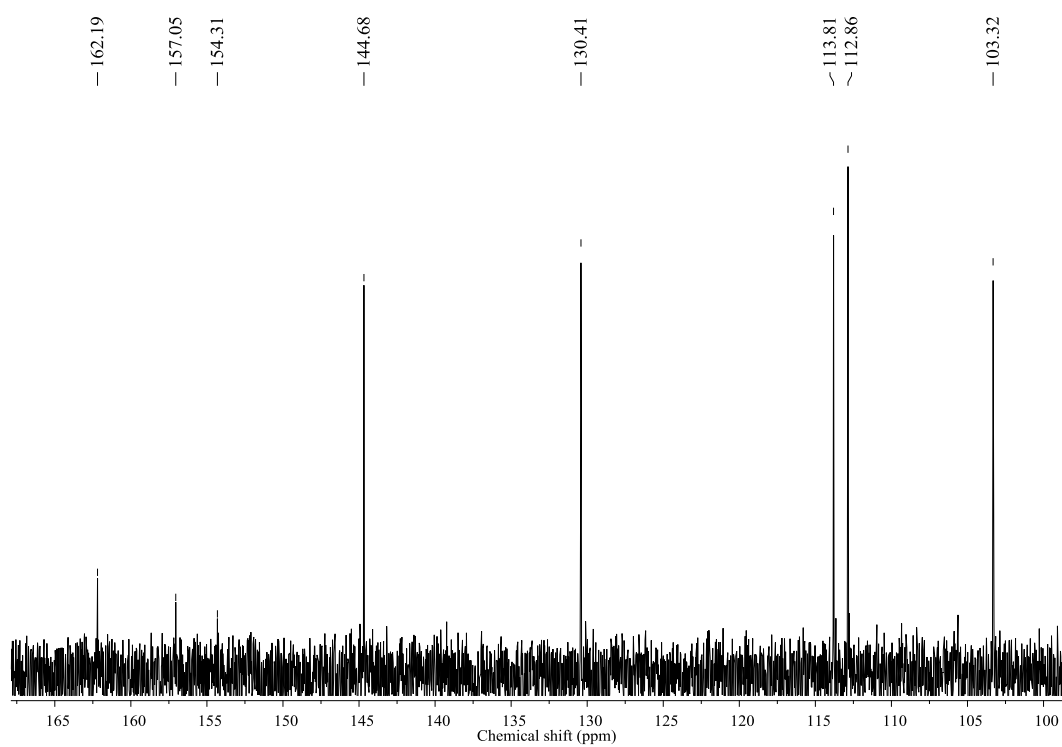**Figure A-18** The ^{1}H-NMR spectrum (CDCl$_3$) of citracridone-I (**9**)

Figure A-19 The ^{13}C-NMR spectrum (acetone-d_6) of umbelliferone (**10**)
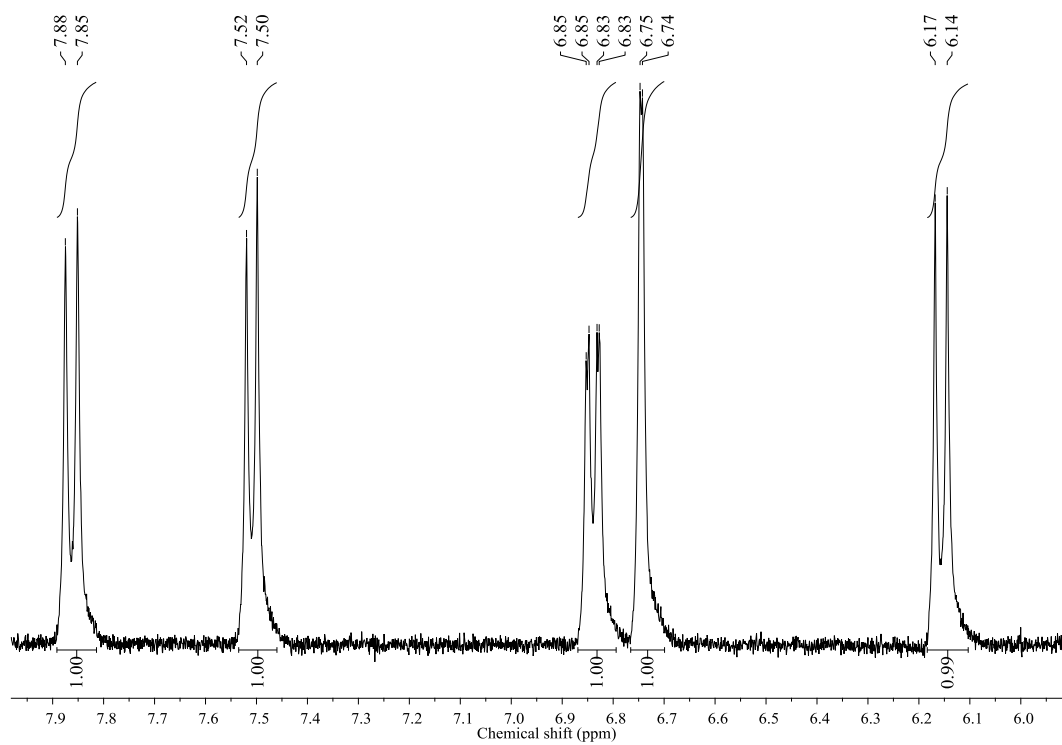

Figure A-20 The ^{1}H-NMR spectrum (acetone-d_6) of umbelliferone (**10**)

VITAE

Mister Setthakorn Niamthiang was born on March 6th, 1987 at Surin Province, Thailand. He graduated with a Bachelor's Degree of Science, in Industrial Chemistry – Analytical Instrumentattions field of Department of Chemistry, Faculty of Science, King Mongkut's Institute of Technology Ladkrabang in 2009 with 2.55 GPA. And then he continued study in Master's Degree of Science, Department of Chemistry, Faculty of Science, Chulalongkorn University. His present address is 552 Moo 6, Tambon Choho, Muang, Nakhon Ratchasima, 30310. Tel. 081-600-3026. His Email address is bom8196@hotmail.com